von KARMAN INSTITUTE
FOR FLUID DYNAMICS

GRANT AF EOOAR 69 - 0065
Final Scientific Report
1 May 1970 - 30 April 1971

THE CALCULATION OF ADIABATIC LAMINAR BOUNDARY LAYER SHOCK WAVE INTERACTIONS IN AXI-SYMMETRIC FLOW PART II - HOLLOW CYLINDER-FLARE BODIES WITH SPIN

by

Roger LEBLANC
Harry P. HORTON
Jean J.GINOUX

VKI TN 73

RHODE-SAINT-GENESE, BELGIUM

JUNE 1971

von KARMAN INSTITUTE FOR FLUID DYNAMICS

GRANT AF EOOAR 69 - 0065
Final Scientific Report
1 May 1970 - 30 April 1971

THE CALCULATION OF ADIABATIC LAMINAR BOUNDARY LAYER SHOCK WAVE INTERACTIONS IN AXI-SYMMETRIC FLOW PART II - HOLLOW CYLINDER-FLARE BODIES WITH SPIN

by

Roger LEBLANC [1]
Harry P. HORTON
Jean J.GINOUX

VKI TN 73

This research has been sponsored in part by the Aerospace Research Laboratories through the European Office of Aerospace Research, OAR, US Air Force, under Grant AF EOOAR 69-0065

---

[1] This work was conducted by Roger Leblanc, Research Assistant at VKI, under the direction of Dr J.J. Ginoux, Professor, and Dr H.P. Horton, Assistant Professor, and will constitute a part of his doctoral thesis.

ACKNOWLEDGEMENTS

The authors wish to thank Mr B. Gautier, who made available to them his computer programme for the calculation of polynomial functions, and Mr M. Riethmuller, who assisted in the development of the computer programme for the interaction calculation.

SUMMARY

This report is concerned with developing a theoretical calculation method for the three-dimensional interaction between a laminar boundary layer and a shock wave, in the case when a constant transverse velocity is imposed, parallel to the shock plane.

The phenomenon is studied on an adiabatic axi-symmetric body consisting of a hollow circular cylinder with a flare. The transverse velocity is generated by the rotation of the body about its axis of symmetry which is aligned in the main flow direction.

The calculation procedure is derived from the two-dimensional integral method of Lees and Reeves. The required relationships between boundary layer integral properties are obtained from similar solutions of compressible axial flow on a rotating cylinder.

It has been established using this theory that a transverse velocity of 10% of the main flow velocity produces a reduction of static pressure in the interaction region of about 2%. This result agrees with wind tunnel measurements made at M = 2.21. On the basis of this agreement, theoretical predictions are made for interactions with larger transverse velocities . It is found that, when the transverse velocity reaches 100% of the main flow velocity, a 10% increment in pressure is predicted.

TABLE OF CONTENTS

LIST OF FIGURES

LIST OF SYMBOLS

a	axial velocity profile parameter, eqs. (28a) and (28b); also speed of sound
$a_{ij}, b_i, b_{ij}, B_i, C_i, D_i$	coefficients in eqs. (30), defined in eqs. (31)
b	transverse velocity profile parameter, eq.(29)
C	Chapman constant, eq. (19)
C_f	skin friction coefficient
C_p	specific heat of gas at constant pressure
D	determinant of system of eqs. (30), defined by eq. (31)
f, g	functions defined by eq. (27c); also Falkner-Skan variables, eq. (32)
f_y, F, F_y, h	functions defined by eq. (27c)
$H = C_p T + \frac{1}{2}(u^2+v^2)$	total enthalpy
$\mathcal{H}, \mathcal{H}_y, \mathcal{H}_{sy}, J, J_{sy}$	shape parameters, defined by eq. (27c)
$K = \dfrac{\beta C M_\infty}{R_{\delta^*_{si}} M_e}$	
$K_1 = v_0/u_\infty$ $K_2 = K_1^2 m_\infty/(1+m_\infty)$ $K_3 = K_2(1+m_e)/m_e$	spin parameters
L	length of cylinder ahead of flare
m	exponent of S for similar solutions
$m = \frac{1}{2}(\gamma-1)M^2$	(with suffix)
$M = u/a$	Mach number
N_1, N_2, N_3	functions defined in eq. (31)
p	static pressure
P	axial skin friction parameter, eq. (27c)

P_1, P_2, P_3, P_4	perturbation functions, eq. (36)
P_y	transverse skin friction parameter, eq. (27c)
Pr	Prandtl number
$Q = \frac{\delta^*_{si}}{r_w} \frac{dr_w}{ds}$	divergence parameter
r	radial distance from the body axis
r_w	local radius of body
R	gas constant
R	axial dissipation parameter, eq. (27c)
R_y	transverse dissipation parameter, eq. (27c)
$Re_u = u_\infty/\nu_\infty$	unit Reynolds number
$R_{\delta^*_{si}} = \delta^*_{si} Re_u$	displacement thickness Reynolds number
s	ordinate along surface generator
S	transformed ordinate along surface generator
T	static temperature
T_1, T_2	functions defined by eq. (34a)
u, v, w	longitudinal, transverse and normal velocity components, measured in (s, y, z) directions
U	transformed u-component of velocity
$v_0 = \Omega r_w$	transverse velocity of surface
x	ordinate along axis of body
y, z	transverse and normal coordinates, see Sketch p.4
Z	transformed normal coordinate
α, σ	see eq. (34)
$\beta = 2m/(m+1)$	Falkner-Skan pressure gradient parameter
$\beta = a_e p_e / a_\infty p_\infty$	
$\gamma = c_p/c_v$	ratio of specific heats of gas at constant pressure and constant volume
δ	flare or ramp angle
δ	boundary layer thickness (at which $u/u_e = 0.99$)
δ^*_s	displacement thickness of axial flow, eq.(16)
δ^*_{si}	transformed displacement thickness of axial flow, eq. (27a)
δ^*_{yi}	transformed displacement thickness of transverse flow, eq. (27a)

δ_u	velocity thickness, eq. (16)
ε	perturbation used to initiate interaction solution
η	independent variable of Falkner and Skan, eq. (32a)
$\theta_s, \theta_y, \theta_{sy}$	momentum thicknesses, eq. (16)
$\theta_{si}, \theta_{yi}, \theta_{syi}$	transformed momentum thickness, eq. (27a)
$\theta^*_s, \theta^*_{sy}$	kinetic energy thicknesses, eq. (16)
$\theta^*_{si}, \theta^*_{syi}$	transformed kinetic energy thicknesses, eq. (27a)
Θ	inclination of the displacement surface to the body surface
$\mathcal{H} = \delta^*_{yi}/\delta^*_{si}$	ratio of transverse to axial transformed displacement thicknesses
μ	coefficient of viscosity of gas
ν	kinematic viscosity of gas
ρ	density of gas
ψ	stream function, eq. (32a)
ω	spin parameter in similarity eqs (32), defined by eq. (34)
Ω	rate of rotation
$\overline{\chi}$	hypersonic interaction parameter, eq. (35)

Suffices

e	local conditions in the external stream
i	transformed quantity in Stewartson plane
t	stagnation conditions
w	at body surface
WI	weak interaction
o	at start of interaction
∞	undisturbed free stream conditions

INTRODUCTION

The phenomenon of shock wave-boundary layer interaction is frequently encountered on high-speed vehicles (air intakes, flaps, etc.). In hypersonic flow the boundary layer is often laminar and therefore sensitive to the impingement of a shock wave. Regions of separated flow are formed which modify appreciably the distributions of surface pressure and heat transfer.

Shock wave-boundary layer interactions are generally three-dimensional in character, and therefore complex to study. Theoretical and experimental work has thus tended to concentrate on the two-dimensional problem. The two-dimensional theory has reached an advanced stage [1,2,3,4,5], and a large body of experimental results is available [6,7,8].

Only recently, attention has been turned to cases of more practical interest. The important problem of three-dimensional interactions in corners has been treated [9]. The analysis of the flow on a lifting surface fitted with a fin (see sketch) is also very interesting. The interaction between the swept, normal shock wave and the boundary layer on the lifting surface is purely three-dimensional. The present study is concerned with interactions having certain important characteristics in common with this type of interaction.

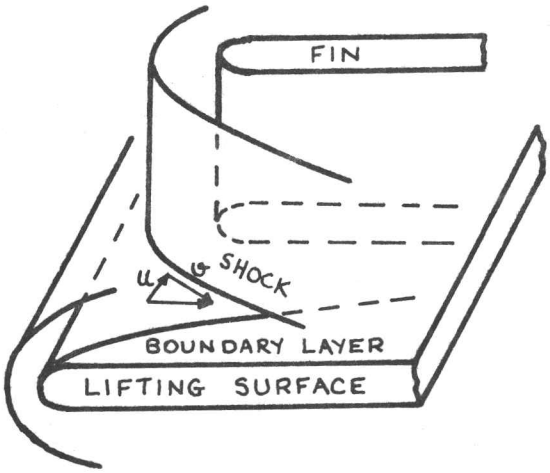

As a first approximation, it is possible to resolve the main stream velocity into its two components u and v, normal and parallel to the shock surface. In fact, it is possible to approach the general three-dimensional problem by the study of interactions produced on a flat plate of infinite span, fitted with a trailing edge flap and placed in sweep to the undisturbed stream (fig. 1a). The use of such a model in a wind

tunnel presents serious difficulties because of end effects, which are particularly large in separated flows.

For this reason we have proposed and constructed, for the experimental part of this research [10], an apparatus consisting of a body of revolution upon which a transverse velocity is produced by spinning the model about its axis of symmetry, which is aligned with the undisturbed stream. Thus, by analogy with the classic two-dimensional flat plate-ramp configuration, we have used a model consisting of a hollow circular cylinder followed by a flare (fig. 1c).

In the present report, a theoretical study is made of the effect of a constant transverse velocity upon the interaction phenomenon, for the purpose of comparison with experimental results. This is an extension to the case with spin of the theoretical study by Horton [11] of interactions on a fixed hollow cylinder-flare configuration.

The method presented here is based on the two-dimensional integral approach of Lees and Reeves [1], as more recently improved by Klineberg [3]. The former method was programmed for an IBM 1130 computer by Gautier [12], this programme having been later adapted by Riethmuller [13] according to Klineberg's modifications. Horton [11] later transformed this programme to treat interactions on axi-symmetric bodies without spin. We here develop the necessary modifications to treat the case with spin.

The first section of this report develops the equations governing interactions with constant transverse velocity. The choice of coordinate system is discussed and the basic boundary layer equations are presented. The transformation of these basic equations to final integral form is discussed. Also, similar solutions for flow over a spinning cylinder are derived, which are used to calculate relations between parameters occuring in the integral equations governing interactions.

The method of numerical solution of the integral equations is discussed in the second section. We briefly discuss the method of calculation of the axi-symmetric external inviscid flow established by Horton [11], based upon the second-order shock-expansion method of Syvertson and Dennis [14], which is directly applicable in the present case. Initial and final conditions for the integration of the equations are discussed, the initial conditions being derived from the analytic solution for weak interaction with spin given by Horton [29] in an accompanying report. We finally recall the iteration and interpolation procedures.

The results of some calculations by the method are presented and discussed in the third section. They are firstly compared with calculations of Horton for the case of a fixed model, and the predicted effect of transverse velocity is noted. Comparison with measurements made without and with spin exhibit similar qualitative behaviour and the same order of magnitude effects. The theory is then used to predict the effect of larger transverse velocities than were obtained experimentally.

1. ANALYSIS

1.1 The basic equations

We discuss in this paragraph the reasons for the choice of the coordinate system used to write the equations governing boundary layer development on a spinning axisymmetric body. The analogy between the energy equation and the momentum equation for the flow in the circumferential direction is shown. The relation existing between the temperature and the velocity components in the boundary layer is deduced, for the adiabatic case.

1.1.1 Choice of coordinate system, and the basic equations

As for interactions on two-dimensional and non-spinning axi-symmetric bodies, we assume that the general boundary layer equations, derived from the concept of Prandtl, are applicable in the case of separated as well as attached flow.

The three-dimensional boundary layer equations are often written in an orthogonal curvilinear coordinate system along and normal to external streamlines. Cooke and Hall [15] discuss the use of this system in detail.

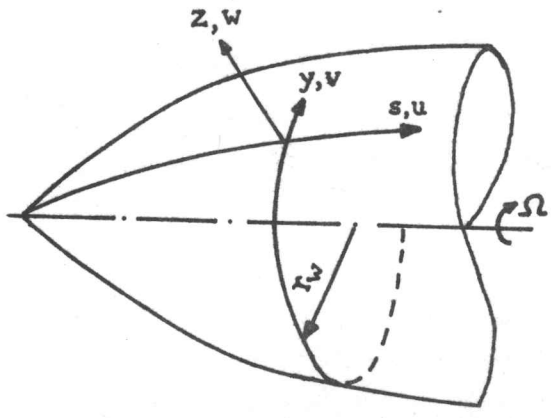

In the present case, it is however simpler to use orthogonal axes fixed in space as shown in the diagram (cf. Mager [15]), such that s is measured along a generator, y is the circumferential transverse coordinate and z is measured normal to the surface. The corresponding velocity components in the boundary layer are u, v, w respectively, v

being the transverse velocity component due to the rotation of angular velocity Ω. $r_w(x)$ is the local radius of the body.

The system of boundary layer equations in this system of axes is, for Prandtl number Pr = 1 :

1. Continuity equation

$$\frac{\partial}{\partial s}(\rho r_w u) + \frac{\partial}{\partial z}(\rho r_w w) = 0 \qquad (1)$$

2. Axial momantum equation

$$\rho\left[u\frac{\partial u}{\partial s} + w\frac{\partial u}{\partial z} - \frac{v^2}{r_w}\frac{dr_w}{ds}\right] = -\frac{\partial p}{\partial s} + \frac{\partial}{\partial z}\left(\mu\frac{\partial u}{\partial z}\right) \qquad (2)$$

3. Transverse momentum equation

$$\rho\left[u\frac{\partial(r_w v)}{\partial s} + w\frac{\partial(r_w v)}{\partial z}\right] = \frac{\partial}{\partial z}\left(\mu\frac{\partial(r_w v)}{\partial z}\right) \qquad (3)$$

4. Energy equation

$$\rho\left[u\frac{\partial H}{\partial s} + w\frac{\partial H}{\partial z}\right] = \frac{\partial}{\partial z}\left(\mu\frac{\partial H}{\partial z}\right) \qquad (4)$$

The boundary conditions are

$$\begin{aligned} &z = 0,\ u = w = 0,\ v = \Omega r_w \quad \text{and} \quad H = H_w \text{ or } \frac{\partial H}{\partial z} = 0 \\ &z \to \infty,\ u \to u_e,\ v \to 0 \qquad \text{and} \quad H \to H_e = C_p T_e + \frac{1}{2}u_e^2 \end{aligned} \qquad (5)$$

According to the boundary layer approximation, $\frac{\partial p}{\partial z} = 0$ so that $\frac{\partial p}{\partial s} \equiv \frac{dp}{ds}$, whilst by symmetry, derivatives with respect to y are zero ($\frac{\partial}{\partial y} = 0$).

The assumption has been made that the boundary layer thickness, δ, is small compared with the local body radius, r_w. Thus transverse curvature effects are neglected, and $r \simeq r_w$ throughout the boundary layer.

The flow on such a body has been studied by Illingworth [17], Chu and Tifford [18] and Schlichting [19].

1.1.2 Relation between temperature and velocity

Chu and Tifford [18] have pointed out the similarity between the equations of y-momentum (3) and of energy (4). A particular solution of the energy equation has the form

$$H = C_p T + \frac{1}{2}(u^2+v^2) = K_1' + K_2' r_w \Omega v \qquad (6)$$

where K_1' and K_2' are constants. From the outer boundary condition (5), it follows that

$$K_1' = H_e$$

In the case of an adiabatic wall considered here $(\frac{\partial H}{\partial z}_w = 0)$ we may find K_2' simply, since

$$C_p \left(\frac{\partial T}{\partial z}\right)_w = 0 = \left(r\Omega \frac{\partial v}{\partial z}(K_2'-1)\right)_w \qquad (7)$$

where C_p is taken to be a constant. Hence, unless $\left(\frac{\partial v}{\partial z}\right)_w = 0$, which is not of practical importance, we have

$$K_2' = 1$$

Then we may put relation (6) in the form

$$\frac{T}{T_e} = 1 + \frac{1}{2C_p T_e}(u_e^2 - u^2 - v^2 + 2r_w \Omega v)$$

or using perfect gas relations

$$\frac{T}{T_e} = 1 + \frac{\gamma-1}{2} Me^2 \left(1 - \frac{u^2+v^2}{u_e^2} + \frac{2r_w \Omega v}{u_e^2}\right) \qquad (8)$$

T is the static temperature, M is the Mach number and the suffix e refers to conditions in the external isentropic flow.

In the case of zero rotation ($\Omega = v = 0$) this reduces to the well-known Busemann integral.

Relation (8) will be used, in conjunction with the perfect gas law, to relate density to velocity in the boundary layer, as will be seen in section 1.2.

1.2 Mathematical treatment of the equations

The similarity, pointed out in the preceding section, between the equations of y-momentum and energy suggests that, for the calculation of an interaction on an adiabatic spinning model, one may calculate the transverse momentum by a method similar to that used by Klineberg to solve the energy equation in the non-adiabatic two-dimensional case.

The problem will thus be treated by the simultaneous solution of four differential equations:

1. The axial momentum equation,
2. The transverse momentum equation,
3. The axial moment-of-momentum equation,
4. The equation coupling the boundary layer and external inviscid flows.

The axial moment-of-momentum equation is obtained by multiplying equation (2) by 2u to give:

$$2\rho u^2 \frac{\partial u}{\partial s} + 2\rho uw \frac{\partial u}{\partial z} - 2\rho uv^2 \frac{1}{r_w} \frac{dr_w}{ds} = 2u\rho_e u_e \frac{du_e}{ds} + 2u \frac{\partial}{\partial z} \left(\mu \frac{\partial u}{\partial z}\right) \tag{9}$$

This equation is necessary only when the system of equations is cast into integral form, by integration across the boundary layer with respect to z, as we shall do.

The coupling equation, first used by Crocco and Lees [20], simply equates the inclination to the wall of the external inviscid flow, Θ, to the slope of a streamline at the edge of the boundary layer, and is obtained by integration of the continuity equation from $z = 0$ to δ :

$$\tan\theta = \frac{v_e}{u_e} = \frac{d\delta_s^*}{ds} - (\delta - \delta_s^*) \frac{d}{ds} (\ell n \rho_e u_e r_w) \qquad (10)$$

However, using the same reasoning as Ref. 11, we neglect the last term to give

$$\frac{d\delta_s^*}{ds} = \tan\theta \qquad (11)$$

so that the slope of the external flow is put equal to the displacement surface slope. This is the coupling equation used by Horton [11] for the case of zero spin, and is applicable without modification to the case with spin since the external flow relations are not affected by spin, and the effective displacement thickness is the axial component δ_s^*.

The calculation of interactions on a spinning body thus requires the solution of four basic equations (2), (3), (9) and (11). The method of solution is similar to that originally conceived by Lees and Reeves [1] for the two-dimensional case. Diagram 1 shows schematically the steps of a calculation.

We shall describe the principal steps in the second section. The mathematical developments which follow are given in detail in ref. 21.

1.2.1 Integral form of the equations

Equations (2), (3) and (9) are integrated across the boundary layer from z = 0 to $\delta(x)$, the outer boundary layer edge, and the w-component of velocity is eliminated using eq. (1). The coupling equation, (11), is already in integral form. The resulting integral equations are

1. Axial momentum integral equation

$$\frac{d}{ds} (\rho_e u_e^2 \theta_s) + \delta_s^* \rho_e u_e \frac{du_e}{ds} + \rho_e u_e^2 (\theta_s + \theta_y) \frac{1}{r_w} \frac{dr_w}{ds} = \mu_w \left(\frac{\partial u}{\partial z}\right)_w \qquad (12)$$

2. Transverse momentum integral equation

$$\frac{d}{ds}(\rho_e u_e^2 \theta_{sy}) + 2\rho_e u_e^2 \theta_{sy} \frac{1}{r_w}\frac{dr_w}{ds} = \mu_w \left(\frac{\partial v}{\partial z}\right)_w \qquad (13)$$

3. Axial moment-of-momentum integral equation

$$\frac{d}{ds}(\rho_e u_e^3 \theta_s^*) + 2(\delta_s^* - \delta_u)\rho_e u_e^2 \frac{du_e}{ds} + \rho_e u_e^3 (\theta_s^* + 2\theta_{sy}^*) \frac{1}{r_w}\frac{dr_w}{ds}$$

$$= 2\int_0^\delta \mu \left(\frac{\partial u}{\partial z}\right)^2 dz \qquad (14)$$

4. Coupling equation

$$\frac{d\delta_s^*}{ds} = \frac{v_e}{u_e} = \tan\Theta \qquad (15)$$

The boundary layer integrals are defined as follows

$$\delta_s^* = \int_0^\delta \left(1 - \frac{\rho u}{\rho_e u_e}\right) dz \qquad \text{- axial displacement thickness}$$

$$\delta_u = \int_0^\delta \left(1 - \frac{u}{u_e}\right) dz \qquad \text{- axial velocity thickness}$$

$$\theta_s = \int_0^\delta \left(1 - \frac{u}{u_e}\right) \frac{\rho u}{\rho_e u_e} dz \qquad \text{- axial momentum thickness}$$

$$\theta_y = \int_0^\delta \frac{\rho v^2}{\rho_e u_e^2} dz \qquad \text{- transverse momentum thickness}$$

$$\theta_{sy} = \int_0^\delta \frac{\rho uv}{\rho_e u_e^2} dz \qquad \text{- cross momentum thickness}$$

$$\theta_s^{**} = \int_0^{\delta} \left(1 - \frac{u^2}{u_e^2}\right) \frac{\rho u}{\rho_e u_e} \, dz$$ - axial kinetic energy thickness

$$\theta_{sy}^{**} = \int_0^{\delta} \frac{\rho u v^2}{\rho_e u_e^3} \, dz$$ - cross kinetic energy thickness

1.2.2 Transformed equations - final system

In the original theory of Lees and Reeves [1] the integral equations are written in the 'incompressible plane' (S,Z) with the aid of the Stewartson [22] transformation. That is, the transformed equations had exactly the same form as those corresponding to an incompressible flow. It is, however, more convenient to leave the s-ordinate untransformed. The Stewartson scalings applied to the velocity u and the normal ordinate z are then

$$dZ = \frac{a_e \rho_e}{a_\infty \rho_\infty} \, dz \qquad \text{and} \quad U = \frac{a_\infty}{a_e} u \tag{17}$$

In the external flow we then have $U_e = \frac{a_\infty u_e}{a_e}$, so that the axial velocity ratio remains invariant:

$$\frac{U}{U_e} = \frac{u}{u_e} \tag{18}$$

Likewise, the transverse velocity ratio $\frac{v}{v_0}$ is invariant under the transformation, where $v_0 = \Omega r_w$.

In addition to relations (17) and (18) we use the Chapman viscosity law

$$\frac{\mu}{\mu_\infty} = C \frac{T}{T_\infty} \tag{19}$$

and the perfect gas law

$$p = \rho R T \qquad (R = C_p - C_v).$$

Since under the boundary layer approximation $\frac{\partial p}{\partial z} = 0$, this relation gives

$$\frac{\rho T}{\rho_e T_e} = 1 \tag{20}$$

We may combine equations (20) and (8) to give the relation between density and velocity. In transformed variables this is

$$\frac{\rho_e}{\rho} = 1 + m_e \left(1 - \frac{U^2}{U_e^2}\right) + K_1^2 m_\infty \left(\frac{1+m_e}{1+m_\infty}\right)\left(2\,\frac{v}{v_0} - \frac{v^2}{v_0^2}\right) \tag{21}$$

where $m_e = \frac{\gamma-1}{2} Me^2$ $\qquad$ $m_\infty = \frac{\gamma-1}{2} M_\infty^2$ (21a)

and $K_1 = \frac{v_0}{u_\infty}$ is the spin parameter, where $v_0 = \Omega r_w$ (21b)

Using the above relations, equations (12) to (15) become:

1. Transformed axial momentum integral equation

$$\mathcal{H} \frac{d\delta^*_{si}}{ds} + \delta^*_{si} \frac{d\mathcal{H}}{ds} + \{(2\mathcal{H}+1) + K_2(2-\mathcal{H}_y)\mathcal{K}\} \frac{\delta^*_{si}}{Me} \frac{dMe}{ds}$$

$$= \frac{\beta C}{R\,\delta^*_{si}} \frac{M_\infty}{Me} P - \{\mathcal{H} + K_3 \mathcal{H}_y\} \frac{\delta^*_{si}}{r_w} \frac{dr_w}{ds} \tag{22}$$

2. Transformed transverse momentum integral equation

$$\mathcal{H}_{sy} \frac{d\delta^*_{yi}}{ds} + \delta^*_{yi} \frac{d\mathcal{H}_{sy}}{ds} + \mathcal{H}_{sy}\mathcal{K} \frac{\delta^*_i}{Me} \frac{dMe}{ds}$$

$$= \frac{\beta C}{R\,\delta^*_{si}} \frac{M_\infty}{Me} \frac{P_y}{\mathcal{K}} - 3\mathcal{H}_{sy}\mathcal{K} \frac{\delta^*_{si}}{r_w} \frac{dr_w}{ds} \tag{23}$$

3. Transformed axial moment-of-momentum integral equation

$$J\frac{d\delta^{**}_{si}}{ds} + \delta^{**}_{si}\frac{dJ}{ds} + \{3J+2K_2(2\mathcal{H}_{sy}-J_{sy})\mathcal{K}\}\frac{\delta^{**}_{si}}{Me}\frac{dMe}{ds}$$

$$= \frac{\beta C}{R_{\delta^{**}_{si}}}\frac{M_\infty}{Me}R - \{J+2K_3J_{sy}\mathcal{K}\}\frac{\delta^{**}_{si}}{r_w}\frac{dr_w}{ds} \qquad (24)$$

4. Transformed coupling equation

$$F\frac{d\delta^{**}_{si}}{ds} + F_y\frac{d\delta^{**}_{yi}}{ds} + \delta^{**}_{si}\frac{d\mathcal{H}}{ds} + (f+f_y\mathcal{K})\frac{\delta^{**}_{si}}{Me}\frac{dMe}{ds} - K_3\delta^{**}_{yi}\frac{d\mathcal{H}_y}{ds}$$

$$= \frac{\beta C}{R_{\delta^{**}_{si}}}\frac{M_\infty}{Me}h - 2F_y\mathcal{K}\frac{\delta^{**}_{si}}{r_w}\frac{dr_w}{ds} \qquad (25)$$

with $\beta = \dfrac{a_e p_e}{a_\infty p_\infty}$, $\quad R_{\delta^{**}_{si}} = \dfrac{\rho_\infty u_\infty}{\mu_\infty}\delta^{**}_{si}$.

K_2 and K_3 are, like K_1, spin parameters being defined by

$$K_2 = \frac{m_\infty}{1+m_\infty}K_1^2, \qquad K_3 = \frac{1+m_e}{m_e}K_2 \qquad (26)$$

The transformed integral thicknesses are defined by

$$\delta^{**}_{si} = \int_0^{\delta_i}\left(1-\frac{U}{U_e}\right)dZ, \qquad \theta_{si} = \int_0^{\delta_i}\left(1-\frac{U}{U_e}\right)\frac{U}{U_e}\,dZ$$

$$\theta^{**}_{si} = \int_0^{\delta_i}\left(1-\frac{U^2}{U_e^2}\right)\frac{U}{U_e}\,dZ$$

$$\delta^{**}_{yi} = \int_0^{\delta_i}\frac{v}{v_0}\,dZ, \qquad \theta_{yi} = \int_0^{\delta_i}\frac{v^2}{v_0^2}\,dZ \qquad (27a)$$

$$\theta^{**}_{syi} = \int_0^{\delta_i}\frac{U}{U_e}\frac{v}{v_0}\,dZ, \qquad \theta^{**}_{syi} = \int_0^{\delta_i}\frac{U}{U_e}\frac{v^2}{v_0^2}\,dZ$$

whilst the ratios between these quantities are defined by

$$\mathcal{H} = \frac{\theta_{si}}{\delta^{**}_{si}} \qquad \mathcal{H}_y = \frac{\theta_{yi}}{\delta^{**}_{yi}} \qquad \mathcal{H}_{sy} = \frac{\theta_{syi}}{\delta^{**}_{yi}}$$

$$J = \frac{\theta^{**}_{si}}{\delta^{**}_{si}} \qquad \mathcal{K} = \frac{\delta^{**}_{yi}}{\delta^{**}_{si}} \qquad J_{sy} = \frac{\theta^{**}_{syi}}{\delta^{**}_{yi}} \tag{27b}$$

Also

$$P = \left[\frac{\partial(U/U_e)}{\partial(Z/\delta^{**}_{si})}\right]_w \qquad P_y = -\left[\frac{\partial(v/v_0)}{\partial(Z/\delta^{**}_{yi})}\right]_w \tag{27c}$$

$$R = \frac{2}{\delta^{**}_{si}} \int_0^{\delta_i} \left[\frac{\partial(U/U_e)}{\partial(Z/\delta^{**}_{si})}\right]^2 dZ$$

$$f = \mathcal{H}\left(\frac{m_e}{1+m_e}\,\frac{\gamma+1}{\gamma-1} + 2\right) + \frac{3\gamma-1}{\gamma-1}, \qquad f_y = K_2\left(\frac{3\gamma-1}{\gamma-1}\right)(2-\mathcal{H}_y),$$

$$F = \mathcal{H} + \frac{1+m_e}{m_e}, \qquad F_y = K_3(2-\mathcal{H}_y) \tag{27d}$$

$$h = \frac{\delta^{**R}_{si}}{C}\,\frac{Me}{M_\infty}\,\frac{1}{m_e}\left(\frac{1+m_e}{1+m_\infty}\right)\tan\Theta$$

The set of four first-order ordinary differential equations (22) to (25) may be solved if uni-parametric families of profiles of U/U_e and v/v_0 are assumed, when the four unknowns become δ^{**}_{si}, Me, a, b, where a and b are the profile parameters.

We assume, following Lees and Reeves [1], that 'similar solutions' of the Falkner-Skan [23] type (see section 1.3) of the basic equations (1) to (4), including lower branch reversed flow solutions of the type found by Stewartson [24], give an

adequate representation of the relationship between integral quantities. Again following Lees and Reeves, the profiles are 'unhooked' from the Falkner-Skan pressure gradient parameter β, whilst, in a manner analogue with Klineberg's [3] treatment of the nonadiabatic two-dimensional case, the axial and transverse (a and b) profiles are decoupled from each other.

The axial velocity profile parameter, a, is defined by

$$a = \left[\frac{\partial(U/U_e)}{\partial(Z/\delta_i)}\right]_w \qquad \text{for attached flow} \qquad (28a)$$

and

$$a = \left[\frac{Y}{\delta_i}\right]_{U/U_e=0} \qquad \text{for separated flow} \qquad (28b)$$

The transverse velocity profile parameter, b, is defined in a similar way to Klineberg's enthalpy profile parameter, and is, for both separated and attached flow

$$b = -\eta_{.99}\left[\frac{\partial(v/v_0)}{\partial(Z/\delta_i)}\right]_w \qquad (29)$$

where $\eta_{.99}$ is the value of the Falkner-Skan ordinate at the boundary layer edge.

The quantities defined in equations (27b) and (27c) may be expressed as polynomials in the variables a and b, so that $\mathcal{H} = \mathcal{H}(a)$, $\mathcal{H}_y = \mathcal{H}_y(b)$, $\mathcal{H}_{sy} = \mathcal{H}_{sy}(a,b)$, $P = P(a)$, $P_y = P_y(b)$, etc. Also $\frac{d\mathcal{H}}{ds} = (\frac{d\mathcal{H}}{da})(\frac{da}{ds})$, $\frac{d\mathcal{H}_y}{db} = (\frac{d\mathcal{H}_y}{db})(\frac{db}{ds})$, etc.

For numerical integration by, for example, the Runge-Kutta method, the system of equations (22) to (25) in the variables δ^*_{si}, Me, a and b may be put in the form

$$\frac{d\delta^{*}_{si}}{ds} = \frac{N_1}{D}$$

$$\delta^{*}_{si}\ \frac{da}{ds} = \frac{N_2}{D} \qquad (30)$$

$$\delta^{*}_{si}\ \frac{db}{ds} = \frac{N_3}{D}$$

$$\delta^{*}_{si}\ \frac{d\ell nMé}{ds} = \frac{N_4}{D}$$

with

$N1 = D1C7 + D3C9 + B2C5$

$N2 = D1C10 + B2C3 - D5C9$

$N3 = B1C1 - D2C10 - B3C3 - D4C7 + B4C5 + D6C9$

$N4 = - B2C1 - D3C10 + D5C7$

$D = D1C1 + D3C3 + D5C5$

with

$B1 = a_{44}b_3 - a_{34}b_4$

$B2 = a_{43}b_3 - a_{33}b_4$

$B3 = a_{42}b_3 - a_{32}b_4$

$B4 = a_{31}b_4 - a_{41}b_3$

$C1 = a_{11}a_{22} - a_{12}a_{21}$

$C3 = a_{11}a_{24} - a_{14}a_{21}$

$C5 = a_{14}a_{22} - a_{12}a_{24}$

$C7 = a_{22}b_1 - a_{12}b_2$

$C9 = a_{24}b_1 - a_{14}b_2$

$C10 = a_{11}b_2 - a_{21}b_1$

and

$a_{11} = \mathcal{H}$

$a_{12} = \frac{d\mathcal{H}}{da}$

$a_{13} = 0$

$a_{14} = (2\mathcal{H}+1)+K_2(2-\mathcal{H}_y)\mathcal{H}$

$a_{21} = J$

$a_{22} = \frac{dJ}{d\mathcal{H}}\frac{d\mathcal{H}}{da}$

$a_{23} = 0$

$a_{24} = 3J+2K_2(2T_1-T_2)\alpha(a)$

$a_{31} = \alpha(a)T_1$

$a_{32} = T_1\frac{d\alpha}{da} + \alpha(a)\frac{\partial T_1}{\partial a}$

$$D1 = a_{33}a_{44} - a_{34}a_{43} \qquad a_{33} = \alpha(a)\,\frac{\partial T_1}{\partial b}$$

$$D2 = a_{32}a_{44} - a_{34}a_{42} \qquad a_{34} = \alpha(a)\,T_1 \quad (= a_{31})$$

$$D3 = a_{32}a_{43} - a_{33}a_{42} \qquad a_{41} = F + F_y\mathcal{K}$$

$$D4 = a_{31}a_{44} - a_{34}a_{41} \qquad a_{42} = F_y\sigma(b)\,\frac{d\alpha}{da} + \frac{d\mathcal{H}}{da}$$

$$D5 = a_{31}a_{43} - a_{33}a_{41} \qquad a_{43} = F_y\alpha(a)\,\frac{d\sigma}{db} - K_3\mathcal{K}\,\frac{d\mathcal{H}_y}{db}$$

$$D6 = a_{31}a_{42} - a_{32}a_{41} \qquad a_{44} = f + f_y\mathcal{K}$$

and with

$$b_1 = KP - Qb_{11} \qquad b_{11} = \mathcal{H} + K_3\mathcal{H}_y\mathcal{K}$$

$$b_2 = KR - Qb_{22} \qquad b_{22} = J + 2K_3T_2\alpha(a)$$

$$b_3 = KP_y - Qb_{33} \qquad b_{33} = 3T_1\alpha(a)$$

$$b_4 = Kh - Qb_{44} \qquad b_{44} = 2F_y\mathcal{K} \qquad (31)$$

K and Q being defined by

$$K = \frac{\beta C}{R\,\delta^*_{si}}\,\frac{M_\infty}{Me} \qquad Q = \frac{\delta^*_{si}}{r_w}\,\frac{dr_w}{ds}$$

$\alpha(a)$, $\sigma(b)$, $T_1(a,b)$ and $T_2(a,b)$ will be defined in the following chapter.

1.3 Similar solutions for a spinning cylinder - Polynomials

1.3.1 The similar solutions

We use, to relate the coefficients in equations (22) to (25), the 'similar solutions' (i.e., solutions depending on a single variable η) for axial flow on a hollow spinning circular cylinder. This procedure again follows the approaches of Lees and Reeves [1] and of Klineberg [3] for related problems.

The boundary layer equations for flow over a spinning circular cylinder are given by equations (1) to (4) with r_w = constant. With this condition they are then identical to those obtained by Crabtree [25] for a swept infinite wing. Only the boundary conditions are different.

The equations for self-similar boundary layer flow on the spinning cylinder of Falkner-Skan type, are [21] :

$$f''' + ff'' + \beta\left(1-f'^2+\omega(2g-g^2)\right) = 0$$
$$g'' + fg' = 0 \qquad (32)$$

for an external velocity distribution in the Stewartson plane of the form $U_e = C_1 S^m$, where S is the transformed axial ordinate. β is related to the exponent m by $\beta = 2m/m+1$. Primes indicate ordinary differentiation with respect to the similarity variable η defined by

$$\eta = \left(\frac{U_e}{\nu_\infty S}\,\frac{m+1}{2}\right)^{1/2} Z \qquad (32a)$$

whilst $f(\eta)$ is directly related to a stream function ψ given by

$$\psi(S,Z) = \left(\nu_\infty U_e S\,\frac{2}{1+m}\right)^{1/2} f(\eta)$$

such that $f' = \frac{U}{Ue}$. The function $g(\eta)$ is defined as $g = \frac{v}{v_0}$, and the boundary conditions are

$$\eta = 0; \quad f = f' = 0, \quad g = 1$$
$$\eta \to \infty; \quad f' \to 1, \quad g \to 0 \qquad (33)$$

The quantity ω appearing in the first of equations (32) is defined by

$$\omega = \left(\frac{\gamma-1}{2}\right) M_0^2,$$

where $M_0 = \frac{v_0}{a_t}$, and $a_t = (\gamma R T_t)^{1/2}$, (34)

T_t being the total temperature of the isentropic external flow.

In the case of incompressible flow, $\omega \to 0$ and the axial profile f', determined from the first of equations (32), becomes independent of the transverse profile g. Coupling between the axial and transverse flows thus only occurs when compressibility effects are important.

The system (32), with the boundary conditions (33), has been solved numerically for a range of values of β and ω. The computer programme used was derived from that given by Klineberg for the calculation of similar solutions for two-dimensional flow with heat transfer. The IBM 1130 computer at VKI was used.

The boundary conditions are given at two 'points' - three conditions are known at the wall $\eta = 0$, and two at the exterior of the boundary layer $\eta \to \infty$. To solve the 5th order system, numerical integration starting at $\eta = 0$ is made using estimates for $(f'')_{\eta=0} \equiv f''_w$ and $(g')_{\eta=0} \equiv g'_w$, and these values are iterated to satisfy the known outer boundary conditions $f'(\infty) \to 1$, $g(\infty) \to 0$.

Figure 2 shows f''_w and g'_w as functions of β for various values of ω. Figure 3 shows velocity profiles for various values of β and ω. The effect of rotation (ω) on the f' and g profiles for a value $\beta = 2.0$ is similar in natura to the effect of sweep for $\beta = 1.0$ shown by Reshotko and Beckwith [26]. That is, for large rates of spin ($\omega = 0.23$ and 0.64) * we observe an overshoot in the axial velocity profile ($f' > 1$) in the outer part of the boundary layer. Cohen and Reshotko [27] observed the same effect in the case of a heated surface. They give the physical explanation that when the wall is strongly heated, the density in the boundary layer is reduced and the fluid is accelerated more rapidly than in the exterior. Reshotko and Beckwith [26] give the same explanation for the overshoot which they observe, remarking that the additional heating is produced by the trans-

* For the experimental conditions considered here ($r_w = 10$ cm, $T_t = 300°K$), these values of ω correspond to 40 and 60×10^3 RPM. Values of RPM quoted henceforth refer to these conditions.

verse wall stress. If this explanation is accepted, it is applicable also in the present case.

1.3.2 Calculation of polynomial functions

The polynomials in a, b, and (a,b) representing the integral quantities defined by relations (27b) and (27c) are calculated by a curve-fit procedure resembling that used by Klineberg [3], starting with a sufficient number of similar solution values, both for attached and separated flows. To each value of β there correspond two similar solution profiles, f' and g, and two parameters a and b characterising these profiles (section 1.2.2). Knowing these profiles, we may calculate $\mathcal{H}$, $\mathcal{H}_y$, etc. for each value of a and b.

We note that the variables η and Z are related by a factor of proportionality such that

$$d\eta = dZ \frac{\eta}{Z} \qquad \text{(cf eq. (32a))}$$

whence

$$\delta^*_{si} = \int_0^{\delta_i} \left(1 - \frac{U}{U_e}\right) dZ = \frac{Z}{\eta} \int_0^{\eta_{.99}} (1-f')\, d\eta$$

$$\theta_{si} = \int_0^{\delta_i} \left(1 - \frac{U}{U_e}\right) \frac{U}{U_e}\, dZ = \frac{Z}{\eta} \int_0^{\eta_{.99}} (1-f')f'\, d\eta$$

We therefore have that

$$\mathcal{H} = \frac{\int_0^{\eta_{.99}} (1-f')f'\, d\eta}{\int_0^{\eta_{.99}} (1-f')\, d\eta} = \alpha \int_0^{\eta_{.99}} (1-f')f'\, d\eta$$

$$\text{where } \alpha = \frac{1}{\int_0^{\eta_{.99}} (1-f')\, d\eta} \qquad (34)$$

$$\text{Also put } \sigma = \int_0^{\eta_{.99}} g\, d\eta$$

when $\mathcal{H}_y = \frac{1}{\sigma} \int_0^{\eta_{.99}} g^2 \, d\eta$ and $\mathcal{K} = \alpha\sigma$

Similarly the quantities $\mathcal{H}_{sy}(a,b)$ and $J_{sy}(a,b)$ may be expressed as

$$\mathcal{H}_{sy} = \frac{T_1}{\sigma}, \qquad J_{sy} = \frac{T_2}{\sigma},$$

where $T_1 = \int_0^{\eta_{.99}} fg \, d\eta$, and $T_2 = \int_0^{\eta_{.99}} fg^2 \, d\eta$ (34a)

The functions $\mathcal{H}(a)$, $\mathcal{H}_y(b)$ and $T_1(a,b)$ are shown in figures 4a, b and c. The continuous line indicates the polynomials (attached and separated) resulting from the curve-fits for $\omega = .0045$, whilst the open circles indicate the discrete points obtained from the similar solutions. For this small rotational speed, the polynomial of $\mathcal{H}(a)$ is almost identical with that of Klineberg for zero heat transfer. The curves of $T_1(a,b)$ are analogous to those of Klineberg ($T(a,b)$) with wall cooling (Klineberg's T is not defined for zero heat transfer). This resemblance is explained by the fact that the f' profiles are almost identical in the two cases, and the transverse velocity profiles and enthalpy profiles resemble each other if the boundary conditions are suitably transformed.

The full circles on figures 4a, b, and c represent discrete similar solution values for a large transverse flow velocity ($\omega = 0.64$, $\Omega = 60{,}000$ RPM). We note that the points lie very close to the polynomials established for small transverse velocity. Thus, although the effect of large rotation is to modify, for example, both $\mathcal{H}$ and a to a marked extent, for a given value of β, nevertheless the functional relation between $\mathcal{H}$ and a remains almost unchanged. This property of the equations has been explained analytically in ref. 28, where it is shown that a change in ω has precisely the same effect as a related change in β, when β is small. Specifically, profiles with spin ω and pressure gradient β_1 are identical with zero spin profiles with pressure gradient β, with $\beta_1 = \beta/(1+\omega)$. Numerically, it is found that for larger values of β

this relation is modified by a multiplicative factor depending upon β. Only for highly accelerated flows does the equivalence break down.

This result enables a considerable simplification in the interaction calculations to be made, in that the polynomials need only be calculated for one value of ω (e.g., $\omega = 0$), and can then be used in interaction calculations for arbitrary ω. This eliminates the inconvenience of the method of Klineberg for the case of heat transfer, in which it was necessary to recalculate the polynomials for each value of wall enthalpy ratio required.

2. SOLUTION OF THE INTERACTION EQUATIONS

2.1 Calculation of the external inviscid flow

The coupling equation, (25), contains the angle θ (by virtue of the definition of h), which is defined as the inclination of external flow streamlines to the surface. This angle must be related to the Mach number in the external flow by some suitable method.

In the two dimensional case the Prandtl-Meyer relation is used. In the present axisymmetric case this relation is not valid. Horton [11] derived, for the case of interactions on an axisymmetric body without spin, an inverted form of the second order shock-expansion method of Syvertson and Dennis [14].

The calculation of the external inviscid flow over a spinning axisymmetric body is directly derived from that without spin. Infact, the external flow relationships are not affected by body spin, and the effective displacement thickness is δ^*_s (the axial component), as mentioned in section 1.2.

A detailed description of this method is given in ref. 11. The validity of the method is shown in fig. 5, where a comparison is made with measurements obtained using a 10° flare, of radius r_c = 100 mm. The good agreement indicates the precision of this simple approximate method.

2.2 Initial conditions for the numerical integration

In order to solve the system of equations (30) governing an interaction, it is necessary to know initial values of the independent variables ($\delta^*_{si_0}$, Me_0, a_0, b_0) to start downstream step-by-step integration.

In the two dimensional case, Klineberg [3] has given analytic expressions for $\delta^*_{si_0}$, Me_0, a_0, derived by series expansion of the interaction equations, for both strong and

weak self-induced interaction on a flat plate. These expressions are used at some point $s = s_0$, the start of the main interaction, as initial conditions to calculate interactions induced by ramps or impinging shocks.

Horton [11], in the case of an axisymmetric body without spin, used the two dimensional weak-interaction expressions of Klineberg. It was shown that this neglect of axisymmetric effects upstream of the main interaction is unimportant when the body radius is sufficiently large.

In the present case, the additional initial value b_0 is required, which does not exist in the two dimensional and zero-spin axisymmetric cases. Furthermore, the transverse flow modifies the axial flow parameters. However, we may assume that for small rates of spin the effect of the transverse flow upon the axial flow is weak. Thus in the case of similar solutions for flow over a spinning cylinder (section 1.2.3) the coupling between the two flows occurs, in equations (32), through a term proportional to ω. For small spin (Ω = 5000 RPM) this parameter is small (ω = 0.0045). Its effect is therefore weak, and its influence upon the weak interaction should be of analogous importance. Hence, for initial conditions with small spin, it should be possible to use those for the non-spin case (i.e., Klineberg's two dimensional values) for δ^*_{si}, Me, and a. The transverse profile parameter b may be taken, as a first approximation, to have its zero pressure gradient (Blasius') value ($b_0 = b_B$), since the weak interaction expansion is an expansion about this condition. This value is given by the similar solutions with $\beta = 0$. The use of these initial values gave good results for small spin rates, as we shall see in section 3.

This procedure is not sufficiently accurate when the spin rate becomes large ($\omega \gtrsim 0.1$). Then it is necessary to derive the full weak interaction expansions, starting with the general equations (22) to (25). This calculation has been carried out by Horton [29]. Equations (22) to (25) were first

written in terms of a new independent variable $\bar{\chi}$, the well-known hypersonic interaction parameter, and a non-dimensional axial displacement thickness Δ ($= R_{\delta^*_{si}} \bar{\chi}/M_\infty^3 C$) and Mach number $\hat{M}$ ($=Me/M_\infty$) were introduced. This led to the system (8) to (11) of ref. 29. Following a similar procedure to that of Kubota and Ko [30], Horton then assumed expansions about the Blasius point of the form

$$\hat{M}_{WI} = 1 + m_1\bar{\chi} + m_2\bar{\chi}^2 + \ldots,$$

$$\Delta_{WI} = \delta_0(1+m_1\bar{\chi}+\ldots),$$

$$a_{WI} = a_0 + a_1\bar{\chi} + \ldots, \qquad (35)$$

$$b_{WI} = b_0 + b_1\bar{\chi} + \ldots,$$

where δ_0, a_0, b_0 are the values for $\bar{\chi} \to 0$ (zero pressure gradient 'Blasius' values), and WI indicates 'weak interaction'.

After substitution of these expansions into the weak interaction integral equations, and identification of powers of $\bar{\chi}$, Horton obtains the coefficients

$$\delta_0 = 1.733, \qquad a_0 = 1.633, \qquad b_0 = 0.470;$$

$$m_1 = -\frac{(\gamma-1)\,(1+m_\infty)}{4M_\infty(M_\infty^2-1)^{1/2}}\left((1+K_1^2)m_{11} + (1+K_1^2+\frac{1}{m_\infty})m_{12}\right),$$

where $m_{11} \equiv \partial\ell_B\delta_0 = 0.662,$

$$m_{12} \equiv \delta_0 = 1.733,$$

$$a_1 = (1+K_2)a_{11}m_1,$$

where $a_{11} = (1-\frac{1}{\partial\ell_B})\Big/(\frac{1}{P}\frac{dP}{da} - \frac{1}{R}\frac{dR}{da})_B = -3.630$

$$\delta_1 = \left(d_{11}(1+K_2)-K_4\right)m_1,$$

where $d_{11} = 2 + \left(\frac{1}{R}\frac{dR}{da}\right)_B$ $a_{11} = 2.111,$

$$b_1 = \frac{\delta_1 + \left(\frac{1}{\alpha}\frac{d\alpha}{da}\right)_B a_1 + m_1K_4}{\left(\frac{1}{P_y}\frac{dP_y}{db}\right)_B - \left(\frac{1}{\sigma}\frac{d\sigma}{db}\right)_B} = \frac{\delta_1 + 0.41a_1 + m_1K_4}{2.294}$$

$$m_2 = \left[\frac{m_\infty}{1+m_\infty} - \frac{1}{2(M_\infty^2-1)}\right] m_1^2,$$

recalling that m_∞, K_1 and K_2 are defined respectively by (21a), (21b) and (26), and where $K_4 = \frac{3\gamma-1}{\gamma-1}\frac{m_\infty}{1+m_\infty}$.

The numerical values quoted were derived from the polynomials for small spin but, using the arguments of section 1.3.2, are equally valid for arbitrary values of spin.

The substitution of these coefficients into the system (35) enables one to calculate the initial conditions, for $\bar{\chi}$ corresponding to s_0, the start of the interaction, necessary for the integration of system (30). It was thus possible to calculate the interaction on a cylinder-flare model spinning at Ω = 60,000 RPM, corresponding to $\omega = 0.64$.

2.3 Iteration and interpolation procedures

2.3.1 Iteration procedure

The system of equations (30), integrated numerically with the initial conditions discussed in section 2.2, exhibits a strong instability, as in the two dimensional and zero-spin axisymmetric cases. As the sketch (next page) shows, a solution of either type I (expansion) or type II (compression) results, the latterbeing the type of present interest. In order to obtain solutions of the desired type, it is necessary to slightly perturb the initial weak-interaction values

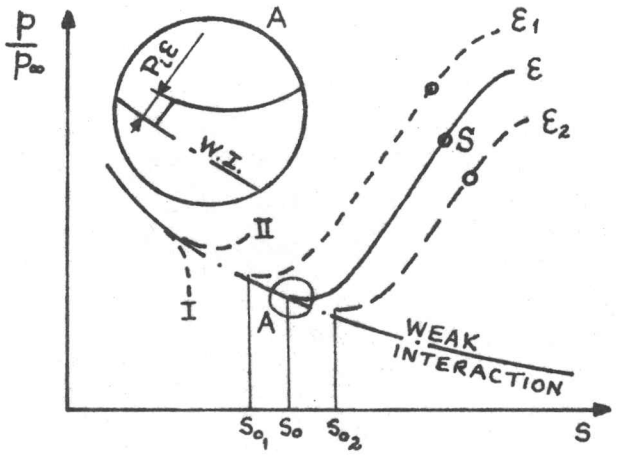

Me_0, $\delta^*_{si_0}$, a_0 and b_0, as described by Ko and Kubota [34] and Klineberg [3]. Horton [29] has derived the form of the perturbation using an analysis similar to that of Ko and Kubota. The expressions for the perturbed variables are :

$$Me = Me_0(1+P_1\varepsilon) \qquad \text{where} \qquad P_1 = \mathcal{H}_0\left(\frac{dJ}{d\mathcal{H}}\right)_0 - J_0,$$

$$\delta^*_{si} = \delta^*_{si_0}\left[1+\left(P_2+K_1^2(P_2+P_1)\right)\varepsilon\right], \qquad P_2 = 3J_0-(2\mathcal{H}_0+1)\left(\frac{dJ}{d\mathcal{H}}\right)_0,$$

$$a = a_0\left(1+P_3(1+K_1^2)\varepsilon\right), \qquad P_3 = J_0(1-\mathcal{H}_0)\Big/\left(d\mathcal{H}/da\right)_0, \qquad (36)$$

$$b = b_0\left(1+P_4(1+K_1^2)\varepsilon\right), \qquad P_4 = \frac{-\left(\mathcal{H}_0(P_1+P_3)+P_2\,\frac{\partial(\mathcal{H}_{sy}\mathcal{K})_0}{\partial a}\right)}{\frac{\partial(\mathcal{H}_{sy}\mathcal{K})_0}{\partial b}}$$

Here, the suffix 'o' indicates the weak interaction solution values calculated for the value of $\overline{\chi}$ corresponding to the value of s_0 chosen.

It is necessary to iterate for s_0 and ε to obtain the solution satisfying the boundary conditions far downstream, as indicated in section 2.3.2. The iteration procedure is identical to that described by Riethmuller and Ginoux [13] for the two dimensional case. An initial value of $\varepsilon = -10^{-3}$ is generally suitable, and the position of the start of interaction s_0 is iterated to the third decimal place. Then s_0 is held constant and further iteration carried out by changing ε. The exact procedure is not critical, because the same solution may be obtained by different combinations of ε and s_0. Thus, referring to the diagram above, starting at $s = s_{0_1}$ we may obtain solution 'ε_1' or 'ε_2' depending upon the value of ε; the same solution ε_2 may be obtained starting at $s = s_{0_2}$ using a value $\varepsilon_2' \neq \varepsilon_2$.

The calculations presented here were carried out using perturbations applied to Me_0, $\delta^*_{si_0}$ and a according to the two dimensional scheme of Ko and Kubota [31], whilst keeping b_0 unperturbed. The rigourous perturbation equations for flow with spin, equations (36), which were later derived, reduce to these relations for $K_1^2 = 0$, $P_4 = 0$. This simplified procedure enabled smooth starting of the integration to be made, but necessitated a doubling of the perturbation ε for large spin rates. The errors introduced into the final results are completely negligeable. However, in future calculations the full scheme (36) should be used.

2.3.2 Downstream conditions and interpolation

According to the correctness of the combination of s_0 and ε for a particular solution in the iterative procedure, the solution may or may not pass through a reattachment; in either case a solution is obtained of either type I (expansion) or type II (new compression). Values of s_0 and ε which are too large lead to type I solutions, and values which are too small to type II. A series of tests on a, Θ, δ^*_{si} and Me allow the determination of the type of solution being generated, so that s_0 or ε may be suitably modified for the next iteration.

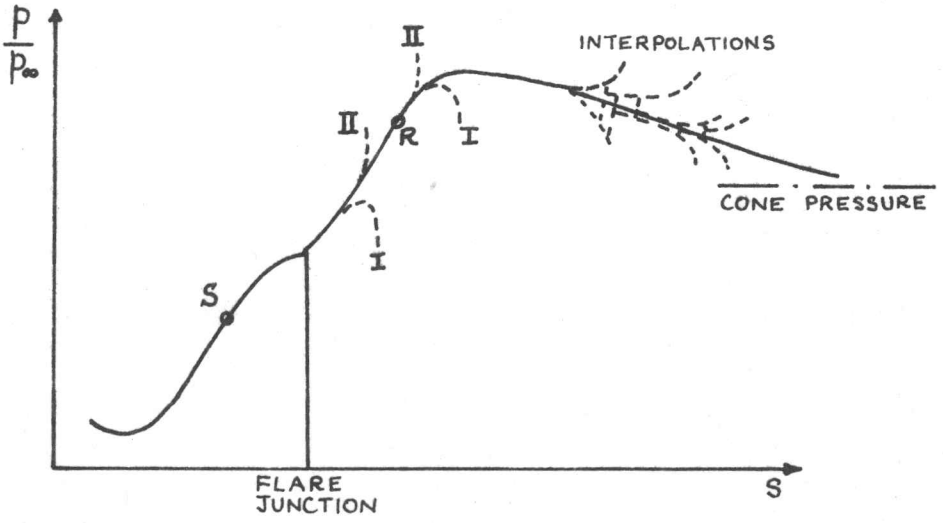

These tests are described in detail for the two dimensional case by Riethmuller [13], whilst Horton [11] has established the tests necessary for the zero-spin axisymmetric case. The latter may be used in the present case without modification.

When the iteration procedure has resulted in two solutions of opposite type which follow each other closely until some distance downstream of reattachment, an interpolation procedure between solutions similar to that described by Riethmuller [13] for the two dimensional case is used to continue the numerical solution as far downstream as desired, still using the same tests to reject solutions as soon as divergence becomes evident.

3. RESULTS AND DISCUSSION

The computer programme for the solution of the system of equations (30) was derived directly from the zero-spin programme of Horton [11], which was itself developed from the programme for two dimensional adiabatic interactions written by Riethmuller [13]. The details of this basic programme are given in ref. 13. We simply remark that it is written in Fortran IV, for use on the IBM 1130 computer of the von Karman Institute.

In the following section we shall discuss the numerical results showing the influence of a transverse flow upon an interaction and we shall compare these predictions with measurements.

3.1 Effect of a weak transverse flow upon the interaction (Ω = 5000 RPM)

Figure 6 shows the predicted effect of a weak transverse flow upon the static pressure distribution in regions of interaction. The pressure is plotted as a function of x, the axial ordinate, in the non-dimensional form $(p-p_{e_0})/p_\infty$, where p_{e_0} is the static pressure at the start of interaction (x_0), and p_∞ is the static pressure of the undisturbed supersonic stream. This form has been adopted in order to eliminate, as far as possible, errors due to the choice of reference pressure [10].

The interaction for the conditions shown in fig. 6a has been verified to be laminar [10]. The flare causing separation has an angle of 7.5° and is placed at an axial distance of 60 mm from the leading edge. The stagnation pressure is 100 mm Hg and the circumferential velocity of the surface is about 10% of the free stream velocity. For the latter condition the cylinder constituting the upstream part of the model, of radius 100 mm, must turn at 5000 RPM.

The transverse flow has a weak effect upon the pressure distribution in the interaction. It tends to reduce the general level of surface pressure. The effect is most pronounced in the separated flow region. The relative pressure increment, $\Delta(p/p_\infty)/(p/p_\infty)$, due to spin at the cylinder flare junction is about 1 %.

The positions of the separation and reattachment points are almost unaltered by the spin, and the influence of spin upon the position of the start of interaction cannot be discerned.

Figures 6b and 6c show results of calculations for two other configurations, the flare being positioned at 40 and 80 mm from the leading edge, and the stagnation pressure remaining unchanged. The effect of spin is similar, in trend and amplitude, to that in the first case.

3.2 Comparison between theory and experiment (Ω = 5000 RPM)

Figures 7a and 7b show comparisons between the results of calculations by the present method and experimental results previously published by Leblanc and Ginoux [10]. The 7.5° angle flare was situated respectively at 60 and 80 mm from the leading edge (7a and 7b), whilst the stagnation pressure was equal to 100 mm Hg. The symbols represent the values obtained experimentally, those for Ω = 5000 RPM indicating measurements corrected for the centrifugal forces acting upon the air in the pressure leads. The continuous and dashed lines represent the pressure distribution calculated theoretically.

The theoretical prediction of the effect of the transverse flow upon the pressure distributions shows a variation in the same direction and of similar amplitude to that observed experimentally. The pressure is reduced, as a result of spin, particularly in the vicinity of separation and reattachment.

The validity of the theory is thus established for the case of small transverse velocities and, since no restrictive assumptions concerning the magnitude of the transverse velocity have been made in the theory, we may use it to predict the effect of transverse velocities larger than those obtained experimentally. Some results are given in the following section.

In order to complete the experimental work reported in ref. 10, we have carried out some tests for the transitional regime. The principal results are given in the Appendix.

3.3 Effect of large transverse flow velocity

Having shown that the polynomial functions used in the theory are universally applicable, whatever the value of the spin parameter ω provided that it is not greater than about unity (the upper limit has not been determined), we can calculate interactions for different magnitudes of transverse velocity simply by solving the system of equations (30) with various values of the parameter K_1.

Figure 8 shows the effect, predicted by the theory, of large transverse velocities upon the pressure distribution in an interaction. The variation of $(p-p_{e_0})/p_\infty$ is shown as a function of x for p_t = 100 mm Hg. The transverse flow is produced by spin rates of 5, 30 and 60×10^3 RPM.

The effect of spin rates of 30 and 60×10^3 RPM is in the same direction as for 5×10^3 RPM, but increased in magnitude. For $\Omega = 30\times10^3$ RPM, the magnitude is about 4% at the cylinder flare junction and also of the same order in the region of the pressure peak. For $\Omega = 60\times10^3$ RPM, the effect becomes very marked - of the order of 5% at separation and 10% at reattachment. The redistribution of pressure due to spin, and therefore the change in loading on the flare, is considerable.

Figure 9 shows the trajectories of the variables $a(x)$, $b(x)$, $\delta^*_{si}(x)$ of equations (30) for $\Omega = 0,5$ and 60×10^3 RPM, $\delta = 7.5°$, $L = 60$ mm and $p_t = 100$ mm Hg. (The fourth variable $Me(x)$, is represented by $p(x)$ in fig. 6a for the same conditions). The general form of the curves is similar (except for $b(x)$) with that obtained and discussed in detail by Lees ad Reeves [1] for the two dimensional case. The transverse velocity profile parameter b has a variation similar to that of the enthalpy profile parameter b used by Klineberg [3].

We note the discontinuities in slope of the curves at the cylinder-flare junction, where Θ is discontinuous. Also, $\frac{da}{ds}$ is discontinuous at separation and reattachment because of the difference in definition of this parameter in attached and separated regions.

From the curve of $a(x)$, it will be seen that separation is retarded and reattachment advanced by the large spin. Also, for $\Omega = 60\times10^3$ RPM, the slope of δ^*_{si} is considerably reduced by the spin, which explains the marked reduction in pressure observed in fig. 8.

CONCLUSIONS

The partial differential equations governing boundary layer flow upon a rotating body of revolution in axial flow have been examined. The similarity between the transverse (y) momentum equations and the energy equation leads to a relation, analogous to that of Busemann, between the static temperature and the velocity components u and v in the boundary layer.

This similarity furthermore suggested that the problem of laminar boundary layer - shock wave interactions on such rotating bodies might be solved by a method similar to that used by Klineberg for the calculation of two dimensional interactions with heat transfer, when the energy equation must be solved. To this end, the boundary layer equations have been put in 'integral' form, and have been simplified by means of a compressibility transformation similar to that of Stewartson.

The coefficients occuring in these equations have been established in the form of polynomial functions of two parameters a and b characterising the velocity profiles u and v. To establish these polynomials, 'similar'solutions' for boundary layer flow on a spinning circular cylinder have been calculated. It was found that these polynomials are, to a very close approximation, independent of the spin parameter ω. This is in contrast with the case of heat transfer treated by Klineberg, in which case it is necessary to calculate the set of polynomials for each value of the wall enthalpy ratio.

The initial conditions for the integration were either the two dimensional adiabatic values of Klineberg (plus b equal to its zero pressure gradient value), in the case of small spin rates, or those calculated by Horton for a spinning cylinder, in the case of large spin rates.

This theory has enabled the effect of a transverse flow upon an interaction to be predicted. Cases were chosen

in which the interaction was known to be entirely laminar. For moderate transverse flow velocities (Ω = 5000 RPM) the effect is weak. In general, rotation causes an overall reduction in pressure in the interaction region, of the order of 1 to 2% for Ω = 5000 RPM.

Comparison with experimental results obtained in a complementary study shows that the measured effect of spin is in the same direction and of similar amplitude. This agreement demonstrates the validity of the present method of calculation. It is therefore possible to use the theory to predict the effects of larger spin ratio, impossible to achieve with the existing model.

Such calculations were made for spin ratio of 30 and 60×10^3 RPM. The trend observed at 5000 RPM is considerably amplified. The relative pressure increment due to spin, in the regions of separation and reattachment, is about 3% at 30×10^3 RPM and 10% at 60×10^3 RPM.

For the largest rate of spin, separation is retarded and reattachment advanced.

REFERENCES

1. LEES, L. & REEVES, B.L.: Supersonic separated and reattaching laminar flows. I - General theory and application to adiabatic boundary layer/shock wave interactions. *AIAA Jnl*, vol. 2, No 11, Nov. 1964, pp 1907-1920.

2. HOLDEN, M.S.: Boundary layer displacement and leading edge bluntness effects on attached and separated laminar boundary layers in a compression corner. Part I - Theoretical study. *AIAA Jnl*, vol. 8, No 12, Dec. 1970, pp 2179-2188.

3. KLINEBERG, J.M.: Theory of laminar viscous-inviscid interactions in supersonic flow. Ph.D. Thesis 1968, Caltech, Pasadena, Cal.; also *AIAA Jnl*, vol. 7, No 12, Dec. 1969, pp 2211-2221.

4. NIELSEN, J.N., LYNES, L.L. & GOODWIN, F.K.: Calculation of laminar separation with free interaction by the method of integral relations. Part I - Two dimensional supersonic adiabatic flows. AF Flight Dynamics Lab., TR 65-107, Part I, 1965.

5. REYHNER, T. & FLÜGGE-LOTZ, I.: The interaction of a shock wave with a laminar boundary layer. Stanford U., Div. Mech. Engrg, TR 163, 1966.

6. CHAPMAN, D.R, KUEHN, D.M. & LARSON, H.K.: Investigation of separated flows in supersonic and subsonic streams with emphasis on the effect of transition. NACA TR 1356, 1958.

7. LEWIS, J.E., KUBOTA, T. & LEES, L.: Experimental investigation of supersonic laminar, two dimensional boundary layer separation on a compression corner with and without cooling. *AIAA Jnl*, vol. 6, No 1, Jan. 1968, pp 7-14.

8. GINOUX, J.J.: Supersonic separated flows over wedges and flares with emphasis on a method of detecting transition. VKI TN 47, 1968.

9. BLOOM, M.H., RUBIN, S.G. & CRESCI, R.J.: Three dimensional viscous interactions. PIBAL Rep. 70-40, 1970, Polyt.Inst.of Brooklyn.

10. LEBLANC, R. & GINOUX, J.J.: Influence of cross flow on two dimensional separation. VKI TN 62, 1970.

11. HORTON, H.P.: The calculation of adiabatic laminar boundary layer - shock wave interactions in axisymmetric flow. Part I - Hollow cylinder-flare bodies with zero spin. VKI TN 63, 1970.

12. GAUTIER, B.: Calcul de l'interaction onde de choc - couche limite laminaire incluant le décollement provoqué par une rampe, à l'aide des méthodes intégrales de Crocco-Lees, modifiées par Glick et de Lees-Reeves. U. Libre de Bruxelles, Inst. d'Aéronautique, NT 23A, 1969.

13. RIETHMULLER, M.L. & GINOUX, J.J.: A parametric study of adiabatic laminar boundary layer - shock wave interaction by the method of Lees-Reeves-Klineberg. VKI TN 60, 1970.

14. SYVERTSON, C.A. & DENNIS, D.H.: A second-order shock expansion method applicable to bodies of revolution near zero lift. NACA TR 1328, 1957.

15. COOKE, J.C. & HALL, M.G.: Boundary layers in three dimensions. AGARD R 273, 1960.

16. MAGER, A.: Three dimensional laminar boundary layers. in *Theory of Laminar Flows, Vol. IV: High Speed Aerodynamics and Jet Propulsion*, 1964, Princeton University Press.

17. ILLINGWORTH, C.R.: The laminar boundary layer of a rotating body of revolution. *Phil. Mag.*, vol. 44, 1953, pp 389-403.

18. CHU, S.T. & TIFFORD, A.N.: The compressible laminar boundary layer on a rotating body of revolution. *Jnl Aero. Sci.*, vol. 21, 1954, pp 345-346.

19. SCHLICHTING, H.: Die laminar Strömung an einen axial angeströmten rotierenden Drehkörper. *Ing. Archiv*, vol. 21, 1953, pp 227-244.

20. CROCCO, L. & LEES, L.: A mixing theory for the interaction between dissipative flows and nearly isentropic streams. *Jnl Aero. Sci.*, vol. 19, 1952, pp 649-676.

21. LEBLANC, R.: Effet d'un écoulement transversal sur une interaction onde de choc - couche limite en configuration de révolution. Doctoral Thesis, 1971, VKI-U.Libre de Bruxelles.

22. STEWARTSON, K.: Correlated incompressible and compressible boundary layers. *Proc. Royal Soc. (London)*, Series A, vol. 200, No A1060, 1949, pp 84-100.

23. FALKNER, V.M. & SKAN, S.W.: Some approximate solutions of the boundary layer equations. ARC, R&M 1314, 1930.

24. STEWARTSON, K.: Further solutions of the Falkner-Skan equations.
Proc. Camb. Phil. Soc., vol. 50, 1954, pp 454-465.

25. CRABTREE, L.F.: The compressible laminar boundary layer on a yawed infinite wing.
Aero. Quart., vol. 5, 1954, pp 85-100.

26. RESHOTKO, E. & BECKWITH, I.E.: Compressible laminar boundary layer over a yawed infinite cylinder with heat transfer and arbitrary Prandtl number.
NACA TN 3986, 1957.

27. COHEN, C.B. & RESHOTKO, E.: Similar solutions for the compressible laminar boundary layer with heat transfer and pressure gradient.
NACA TN 3325, 1955.

28. HORTON, H.P., LEBLANC, R. & GINOUX, J.J.: Integral relations for self-similar adiabatic laminar boundary layers with constant transverse velocity.
(to be published, VKI).

29. HORTON, H.P.: Weak viscous interaction on a spinning hollow cylinder body in axial adiabatic supersonic flow.
VKI TN 74, 1971.

30. KUBOTA, T. & KO, D.R.S.: A second order weak interaction expansion for moderately hypersonic flow past a flat plate.
AIAA Jnl, vol. 5, No 10, Oct. 1967, pp 1915-1917.

31. KO, D.R.S. & KUBOTA, T.: Supersonic laminar boundary layer along a two dimensional adiabatic curved ramp.
AIAA Jnl, vol. 7, No 2, Feb. 1969, pp 298-304.

APPENDIX - EFFECT OF TRANSVERSE FLOW UPON A TRANSITIONAL INTERACTION

The results of the theory developed in this report have been compared with measurements obtained previously by the first and last authors [10]. It was verified that the interactions in these tests were fully laminar, the theory being applicable only under this condition.

It was desired to complete these measurements by examining the influence of a transverse flow upon a transitional interaction. It was known [10] that, without spin, the effect of change of Reynolds number is of opposite sense according to whether the interaction is laminar or transitional. Would the effect of rotation, also, be in the opposite sense ?

The tests were carried out with the 10° flare positioned at 40 mm from the leading edge, a configuration which produces the two types of flow (laminar or transitional) according to the unit Reynolds number [21].

Figure A1 shows the effect of rotation upon the pressure in the interaction region when the unit Reynolds number of the free stream is small (corresponding to p_t = 97.2 mm Hg). We note that the transverse flow produces the same "laminar" trend observed for the 7.5° flare (fig. 6a), with a general reduction in pressure level.

The same experimental configuration has been tested at a higher Reynolds number (corresponding to p_t = 172.6 mm Hg). The results are shown in fig. A2. The effect of rotation is now to increase the level of pressure in the region of separation. This trend is thus opposite to that observed in the laminar case.

This result has been confirmed by repeating the tests for the transitional interaction, the 10° flare being placed at 60 mm from the leading edge. The same result was found.

Figure A3 shows the same effect when the flare has an angle of 15°, for L = 60 mm.

In conclusion, it appears that the destabilizing effect of spin upon the boundary layer produces changes in pressure near separation in opposite directions depending on whether the interaction is laminar or transitional. Changes of Reynolds number have a similar effect.

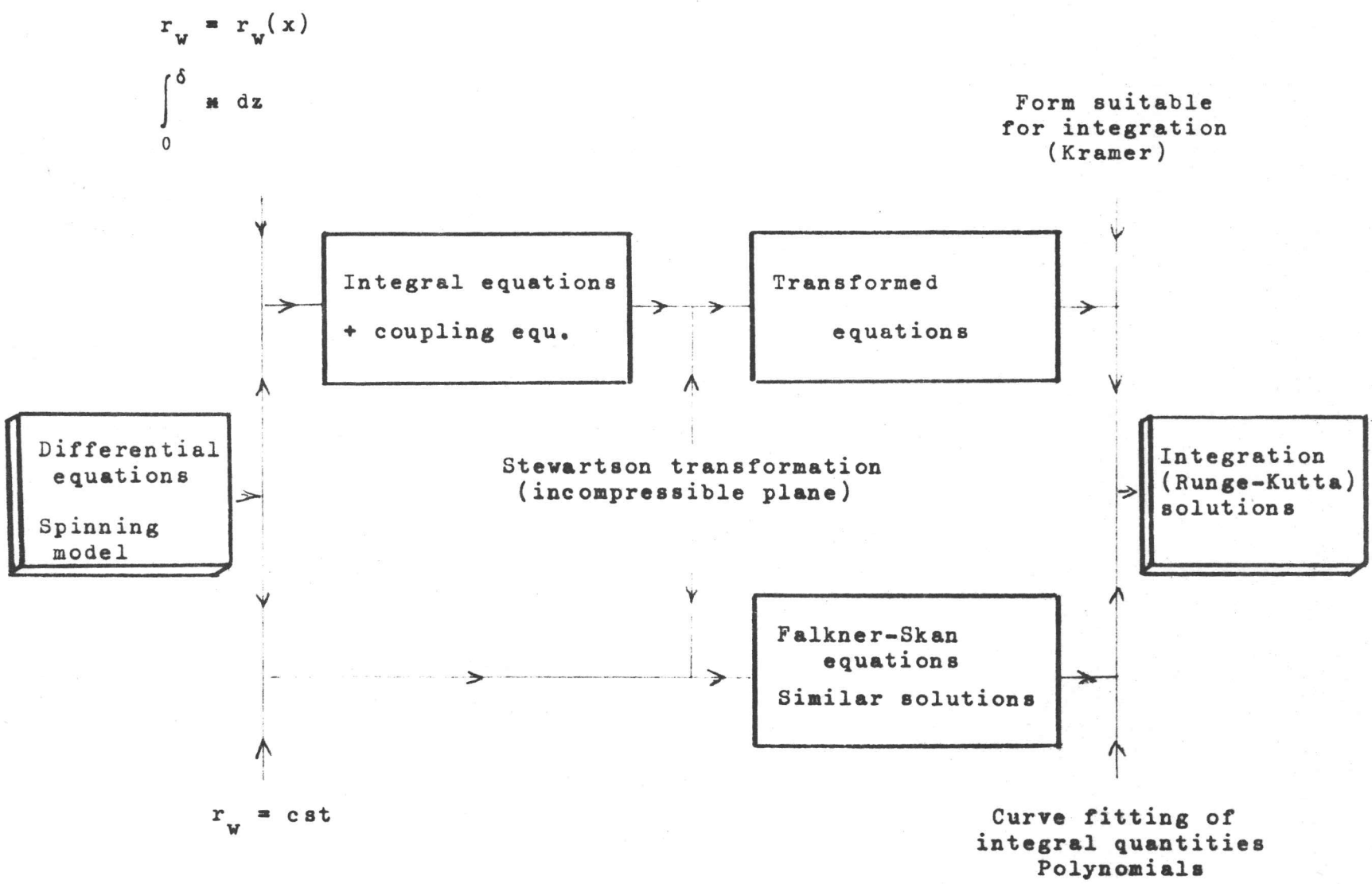

Diagram 1 - Schematic diagram of the method of calculation for spinning body

a) swept wing

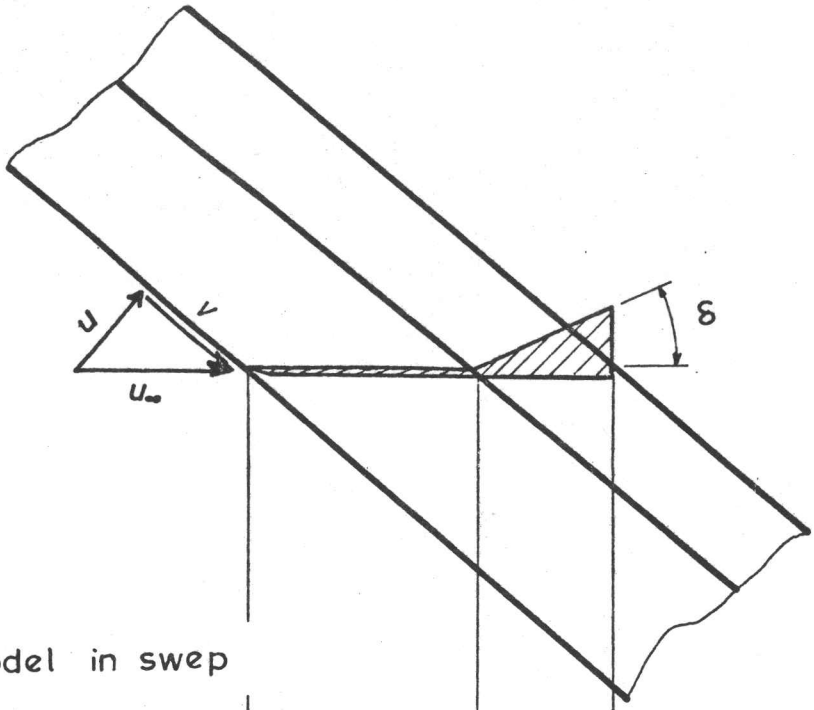

b) 2-D model in swep

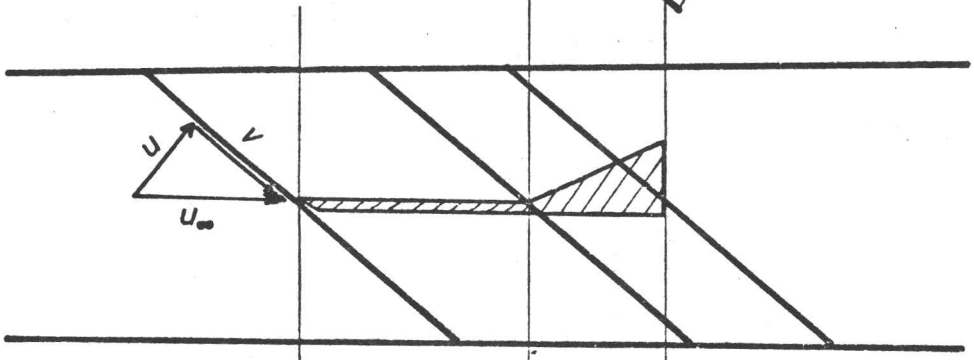

c) axisymmetric rotating model

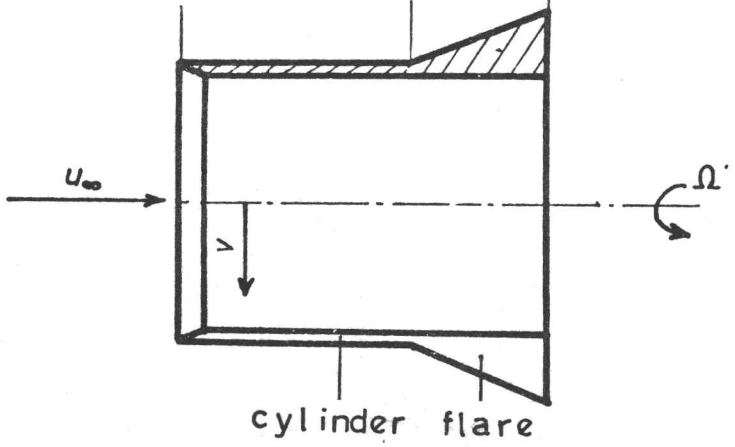

Fig.1 Interaction with cross flow

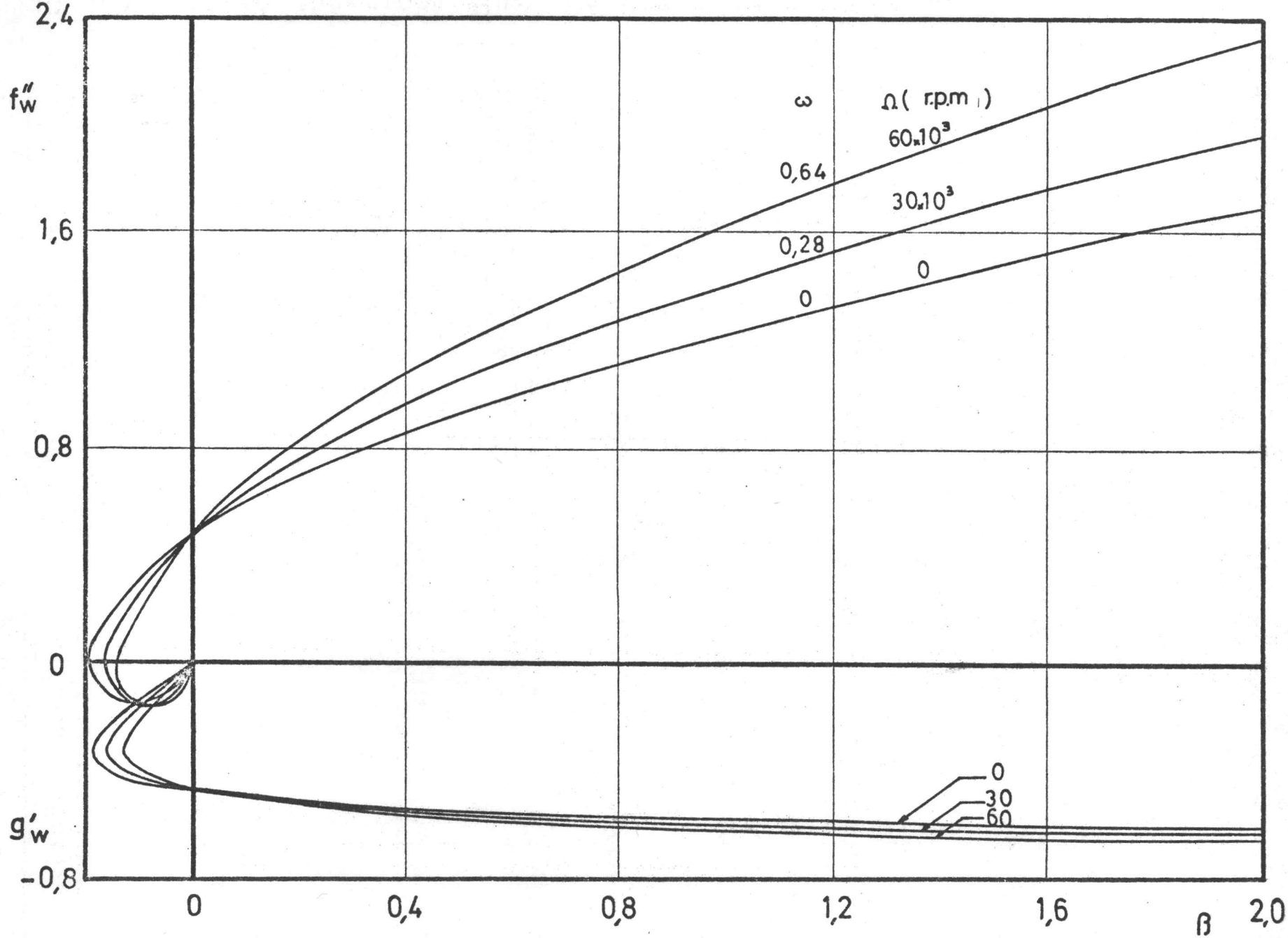

Fig 2 $f''(\beta)$ and $g'(\beta)$

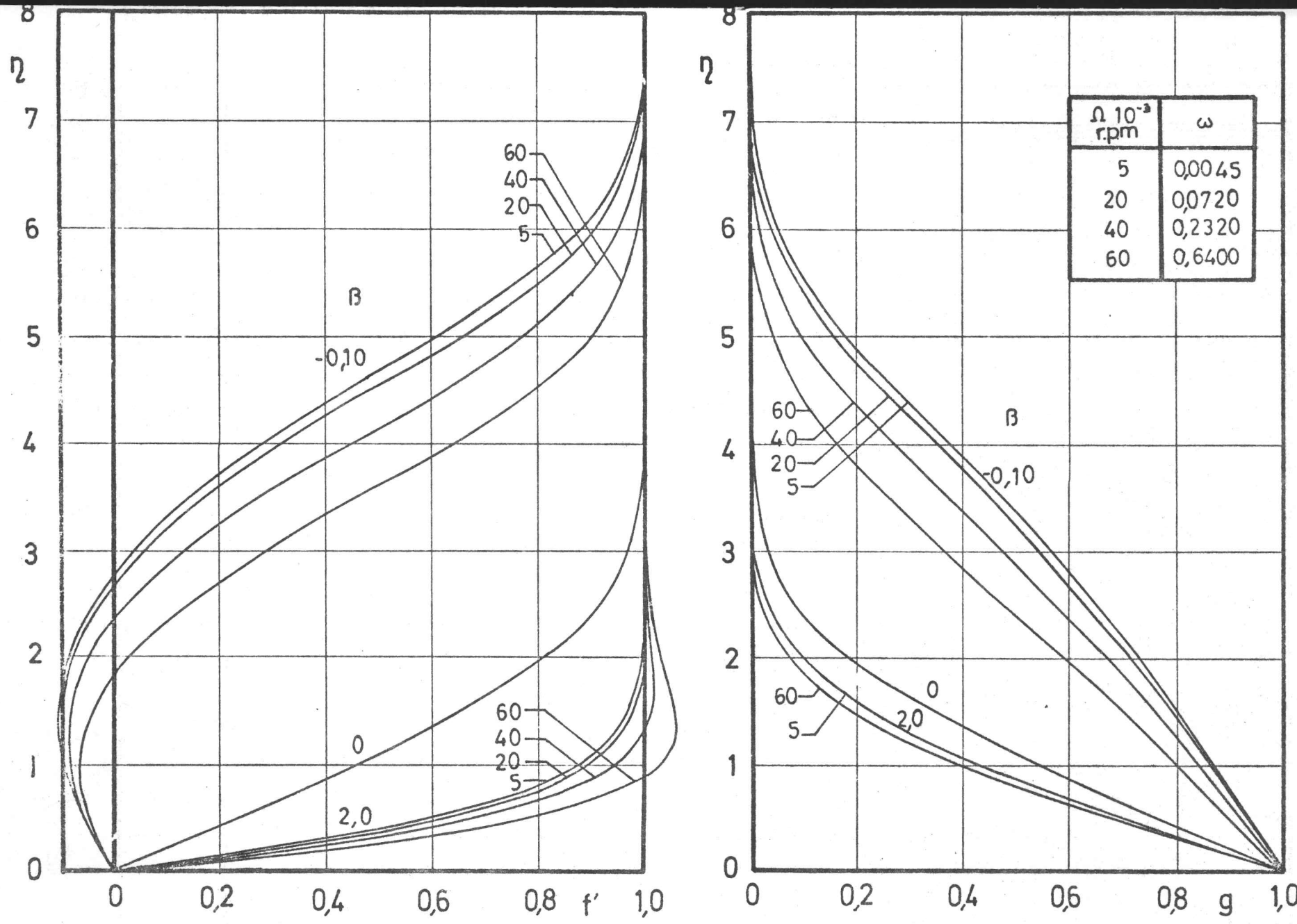

Fig. 3- Effect of the cross flow on the velocity profiles

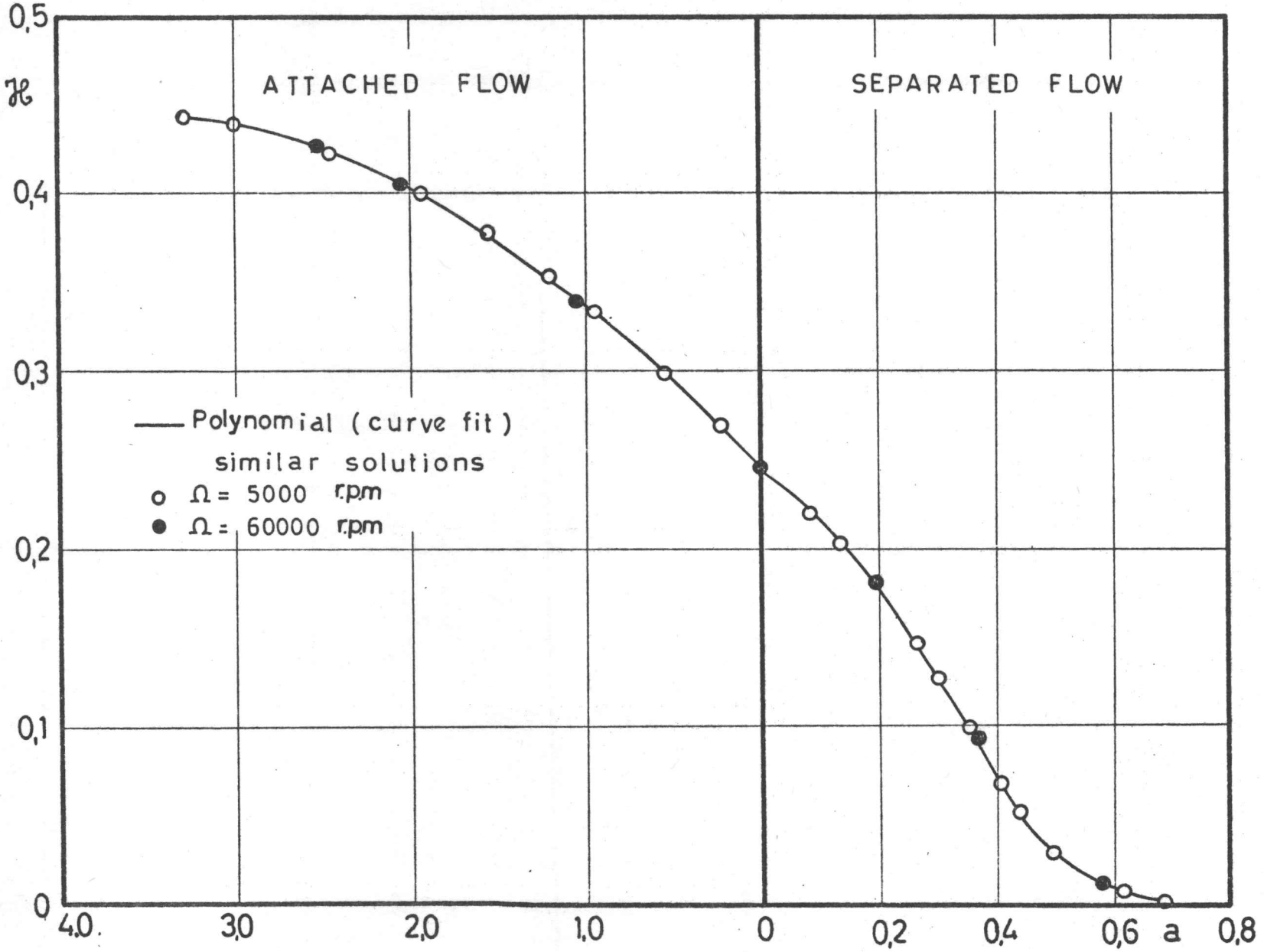

Fig. 4a _ Theoretical $\mathcal{H}(a)$ distribution

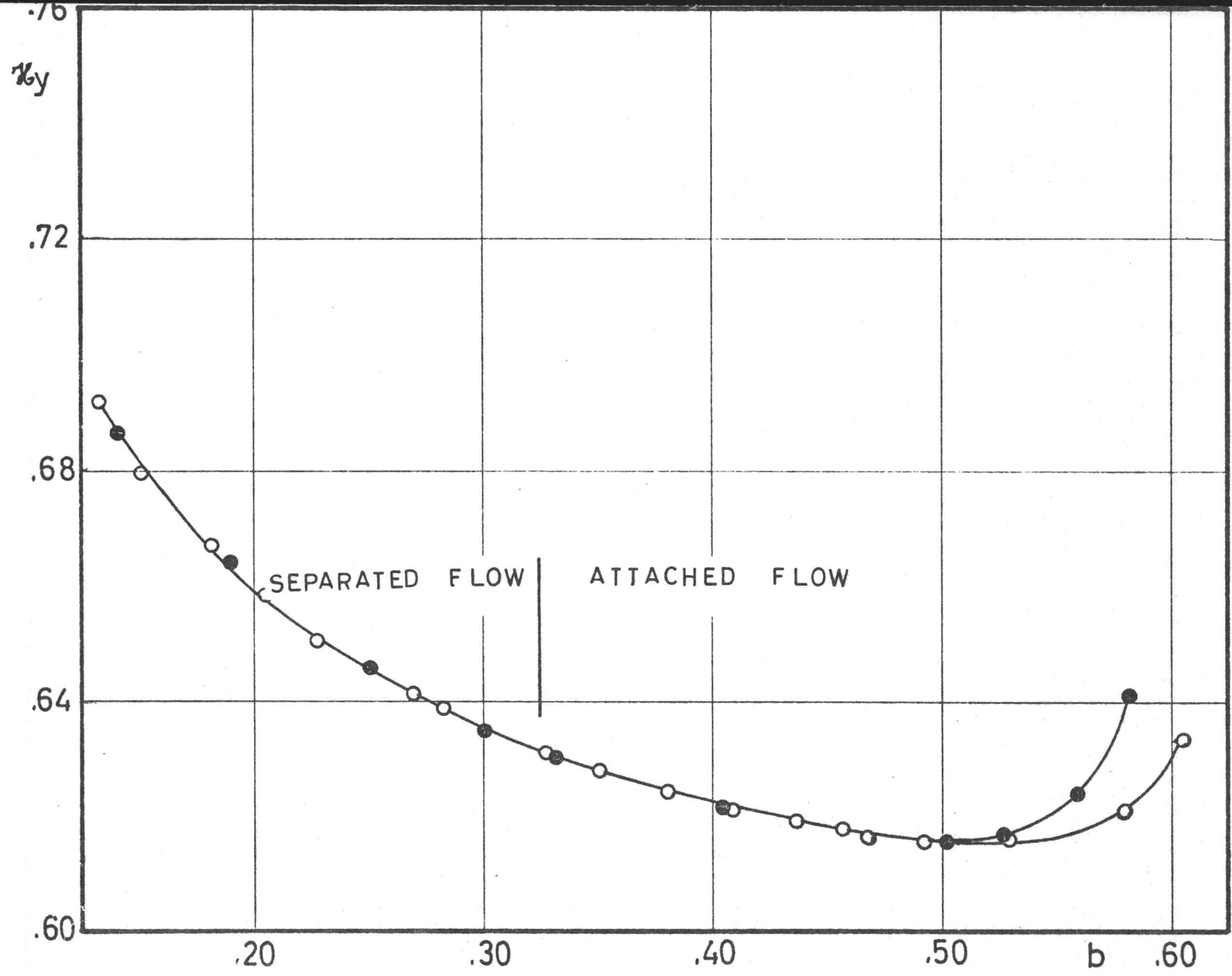

Fig. 4b_ Theoretical $\gamma_y(b)$ distribution

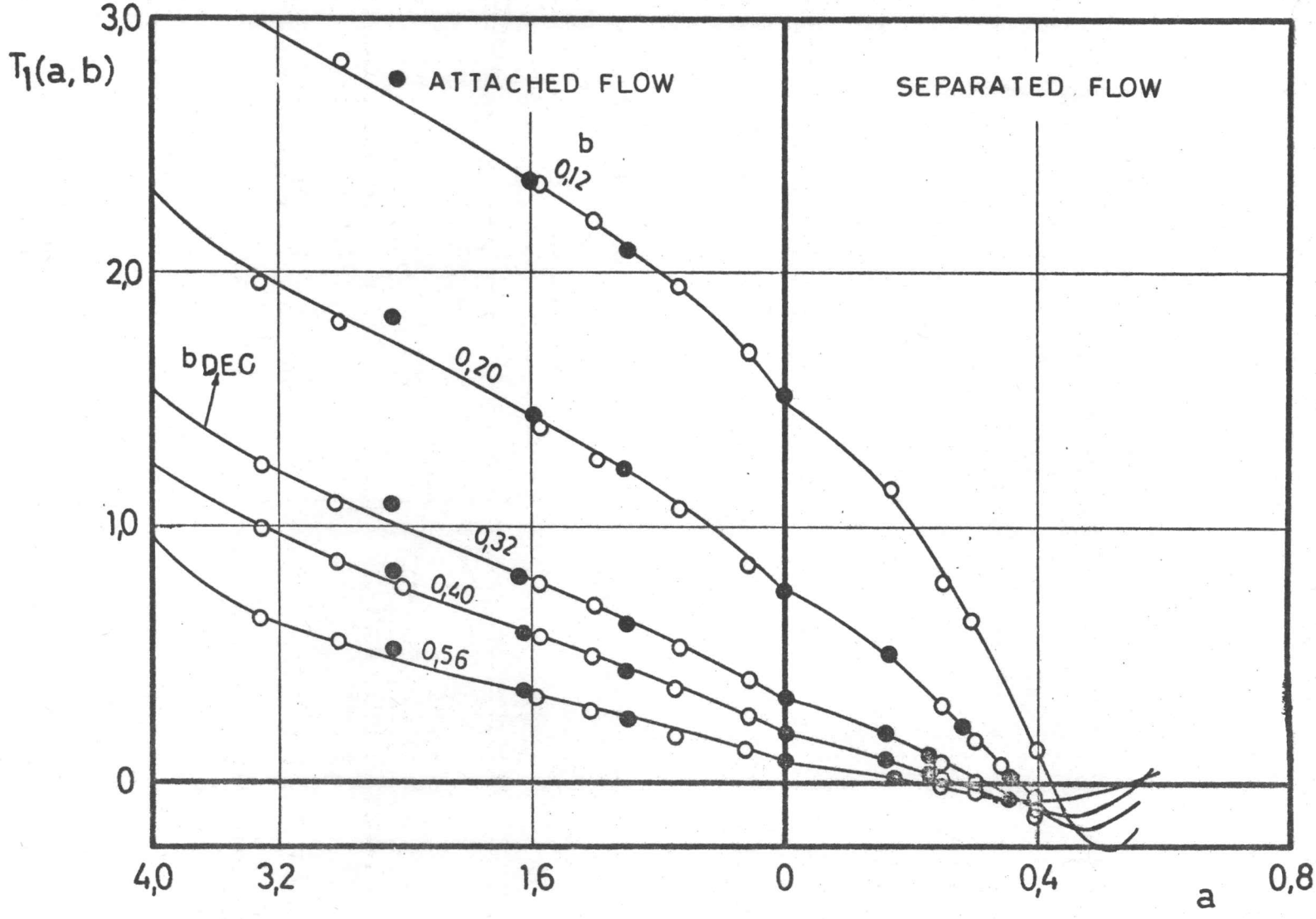

Fig. 4c_ Theoretical $T_1(a,b)$ distribution

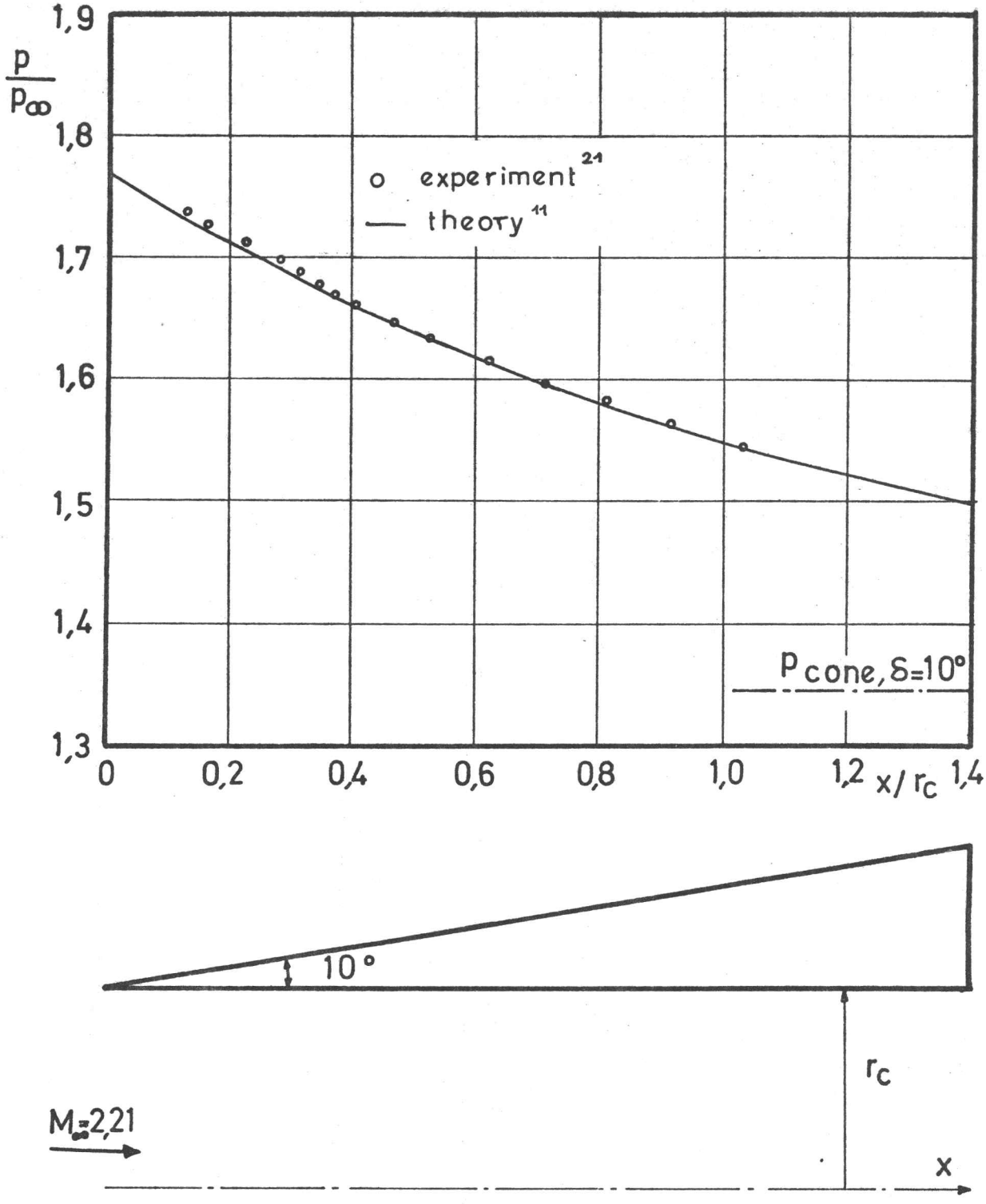

Fig. 5 _ Inviscid pressure on the 10° flare

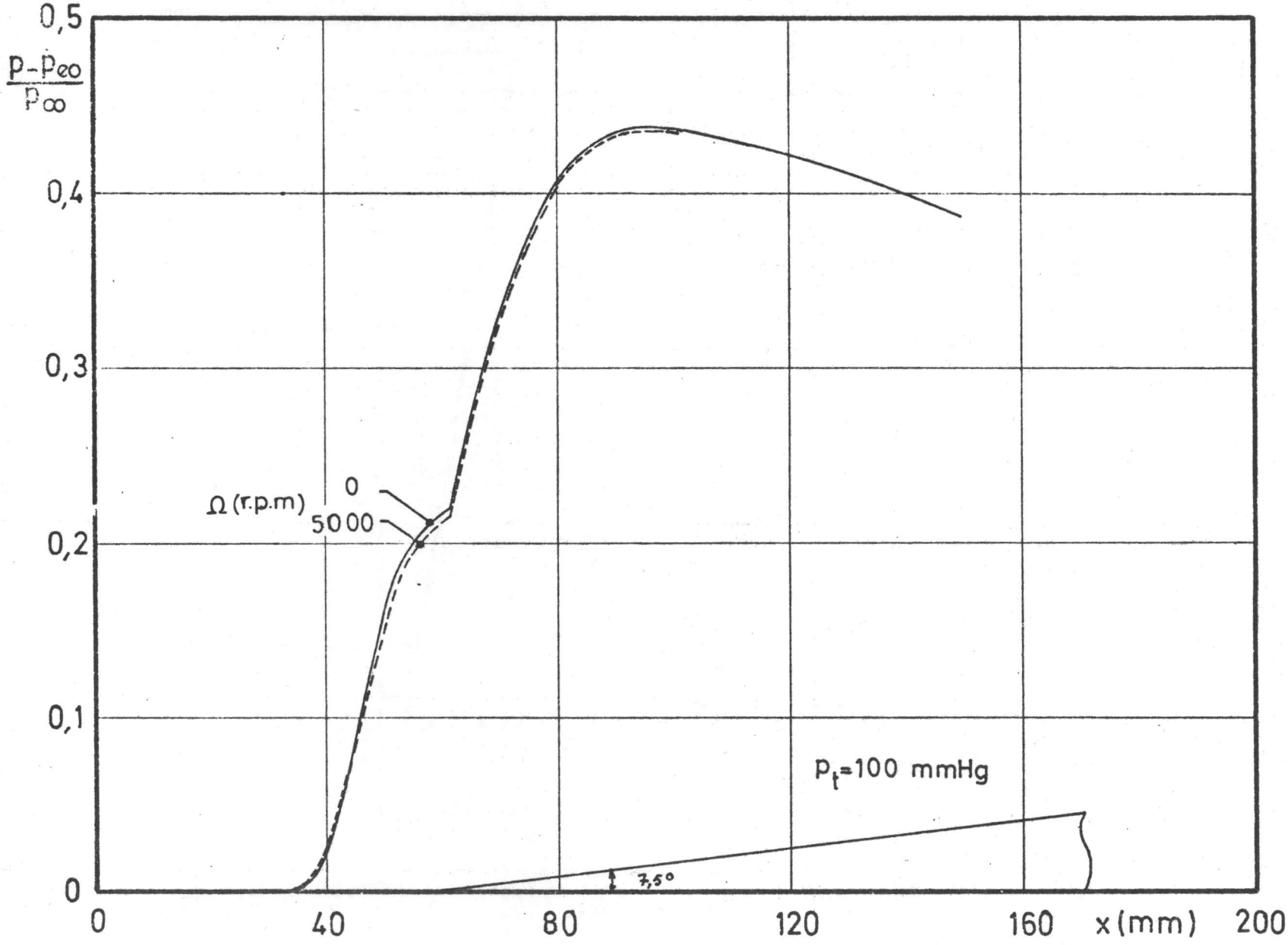

FIG. 6 a _ Effect of the cross flow (theory L_1 = 60 mm)

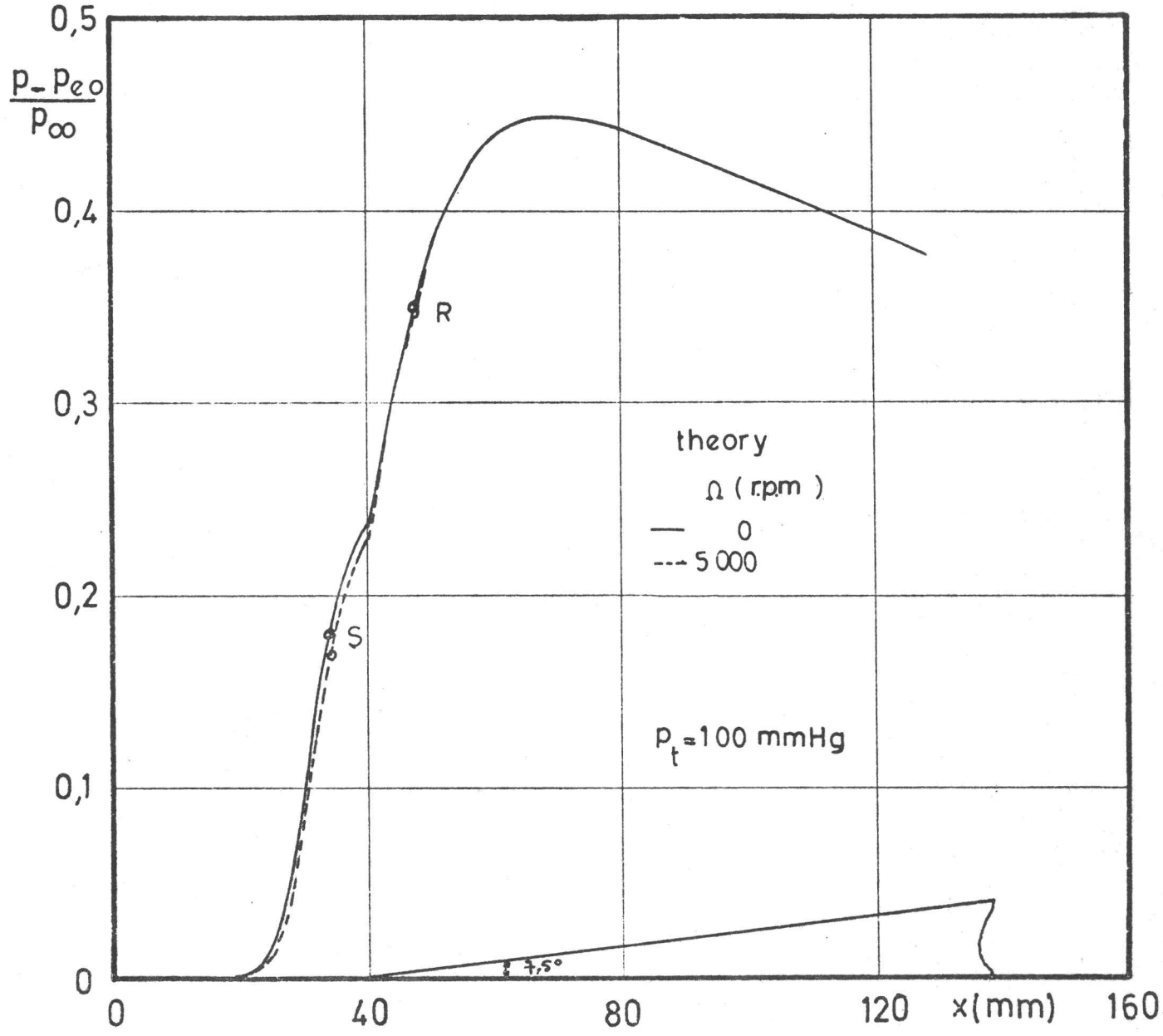

Fig 6b_ Effect of the cross flow (theory, L = 40 mm)

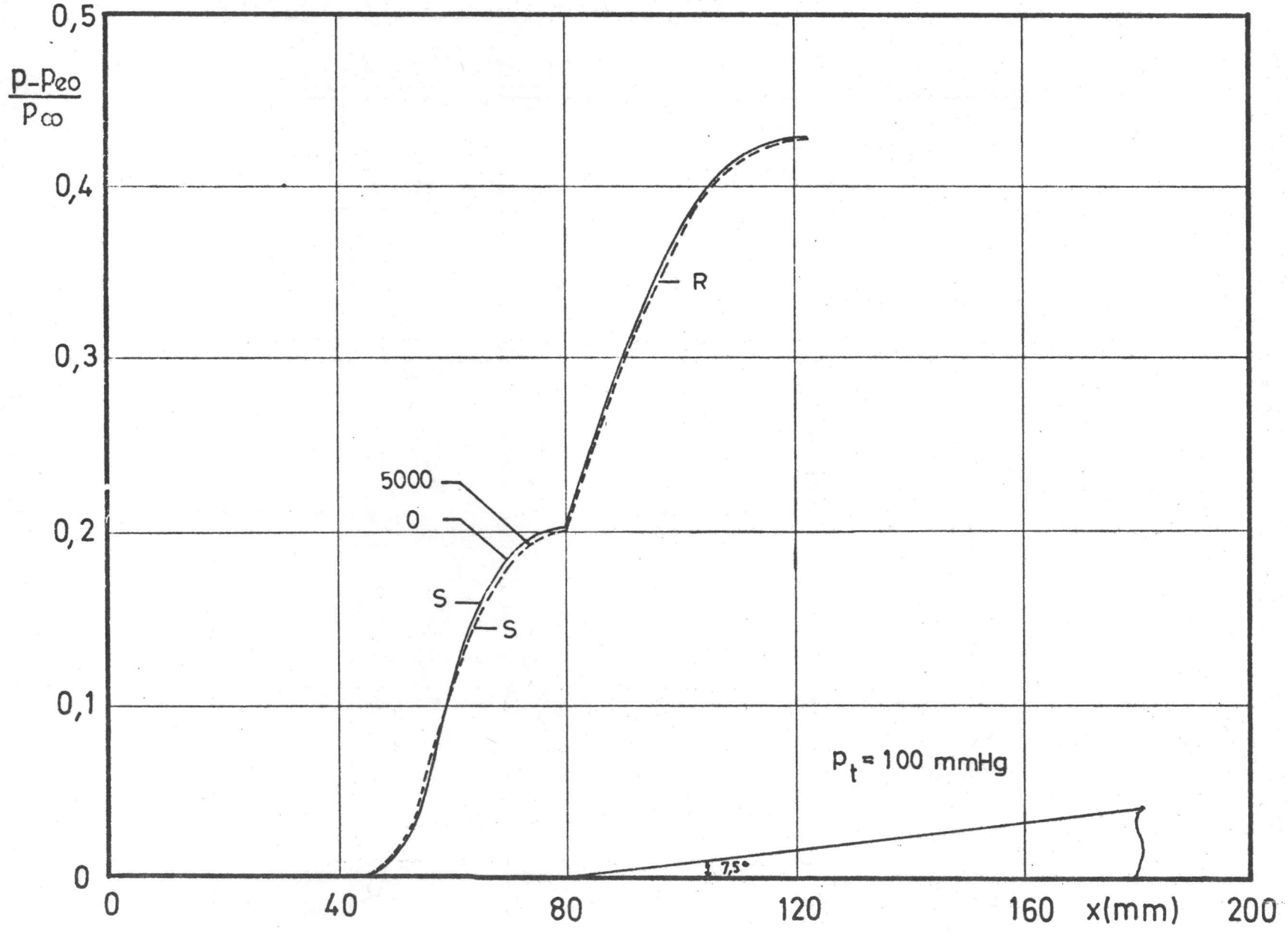

Fig. 6c - Effect of the cross flow (theory, L = 80 mm)

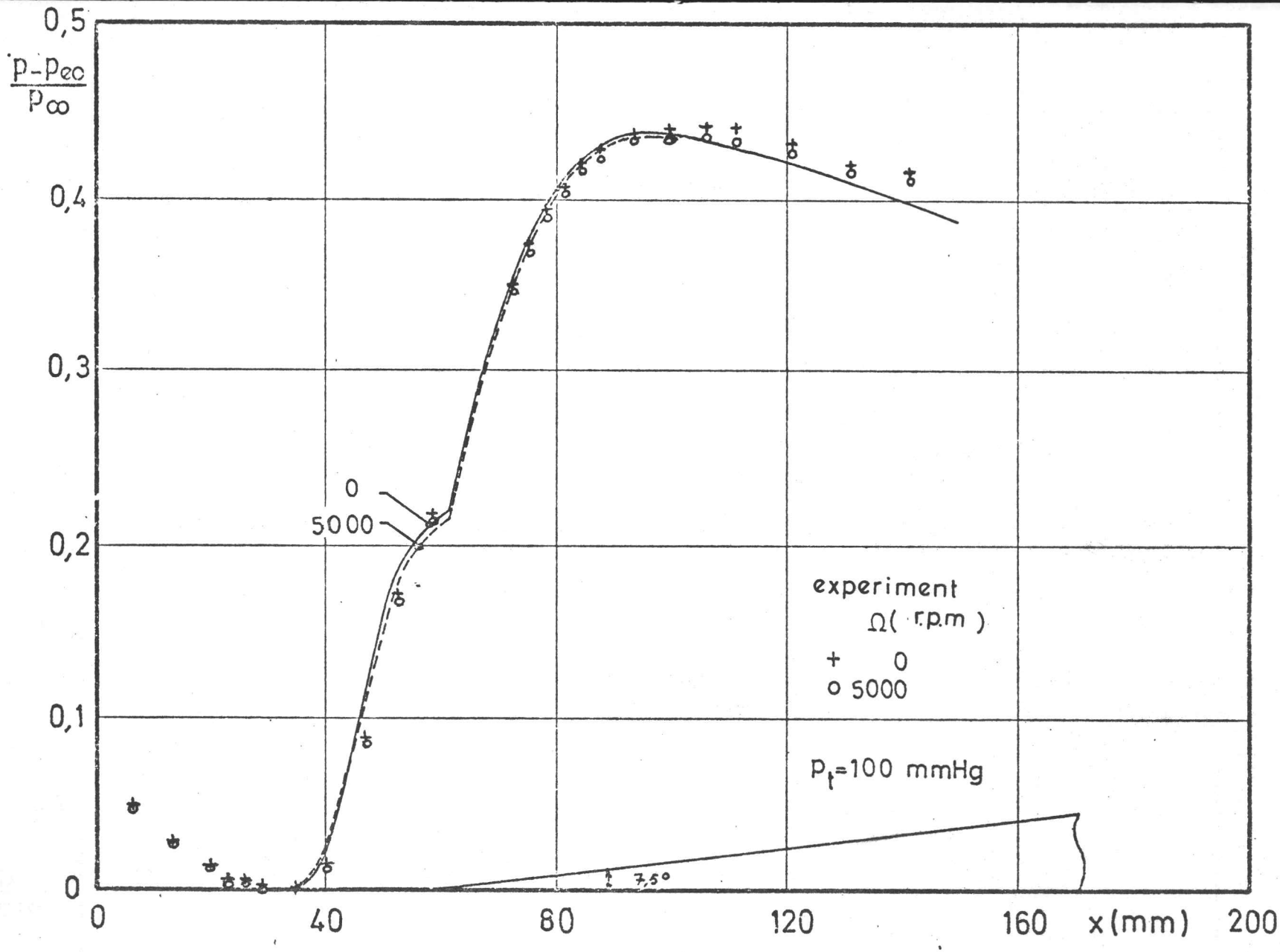

Fig. 7a - Effect of cross flow - Comparison theory-exp. (L=60)

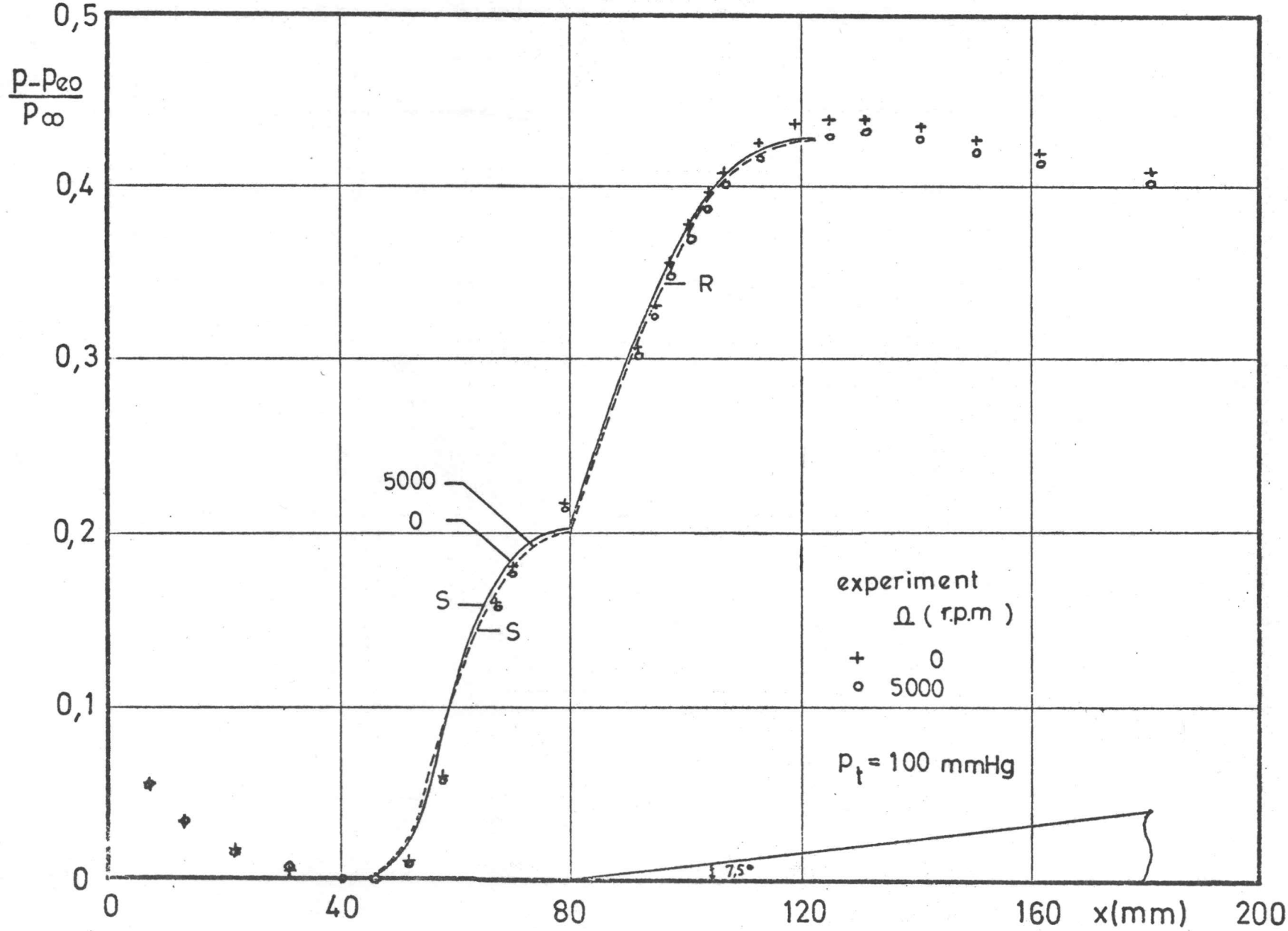

Fig. 7 b - Effect of cross flow - Comparison theory exp (l_1 =80)

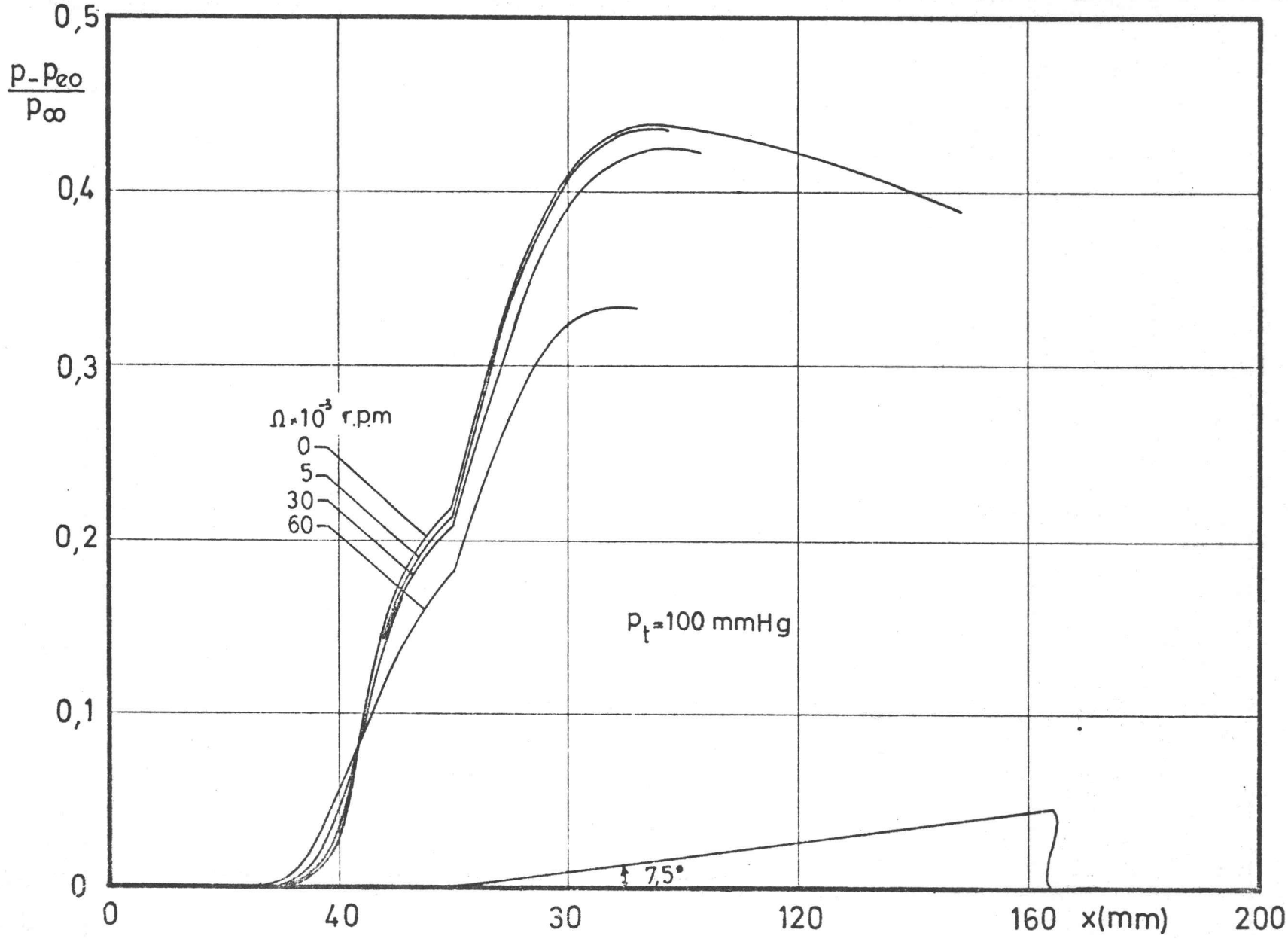

Fig. 8 - Effect of large cross flows

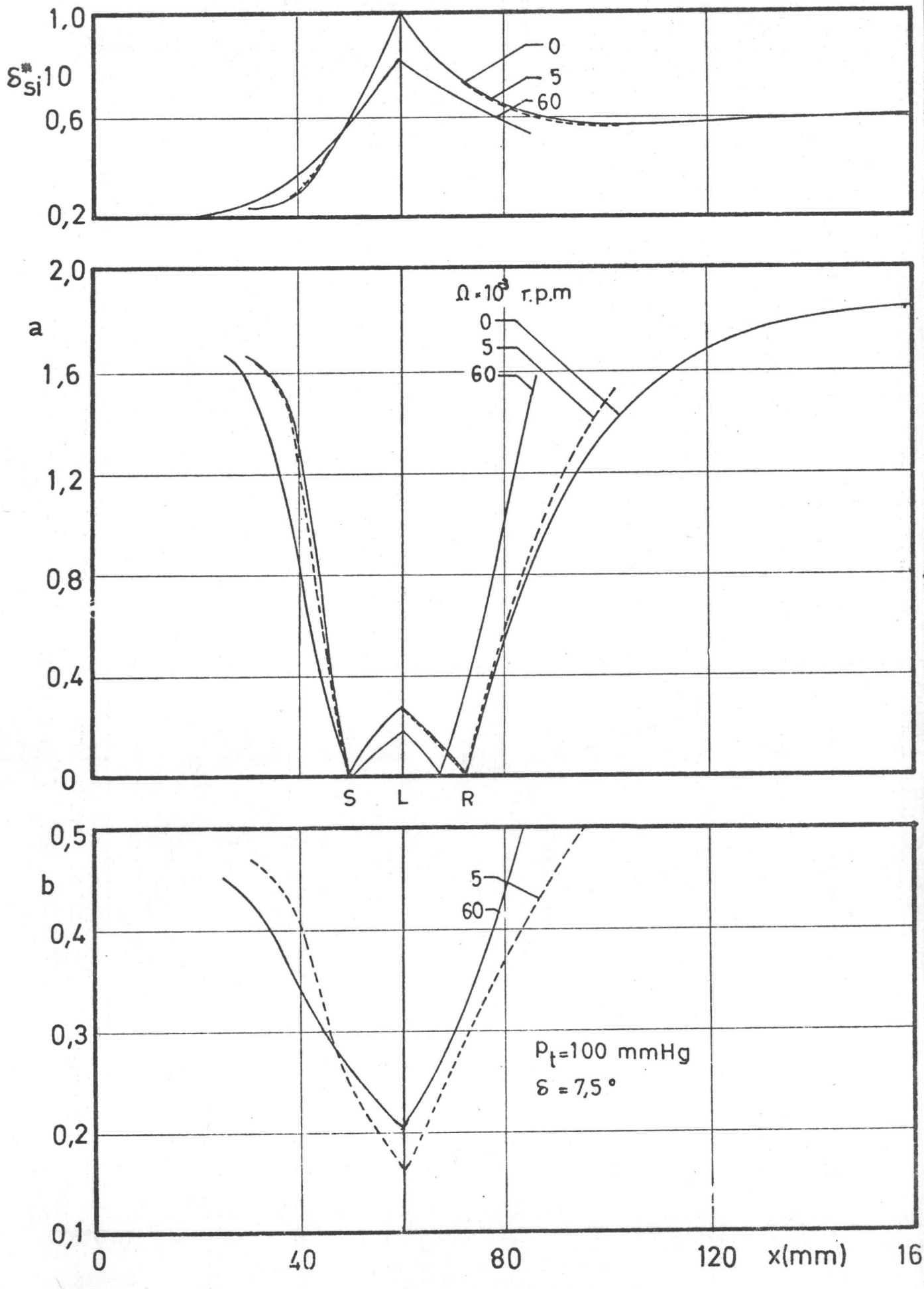

Fig 9 - δ^*_{si} , a and b trajectories

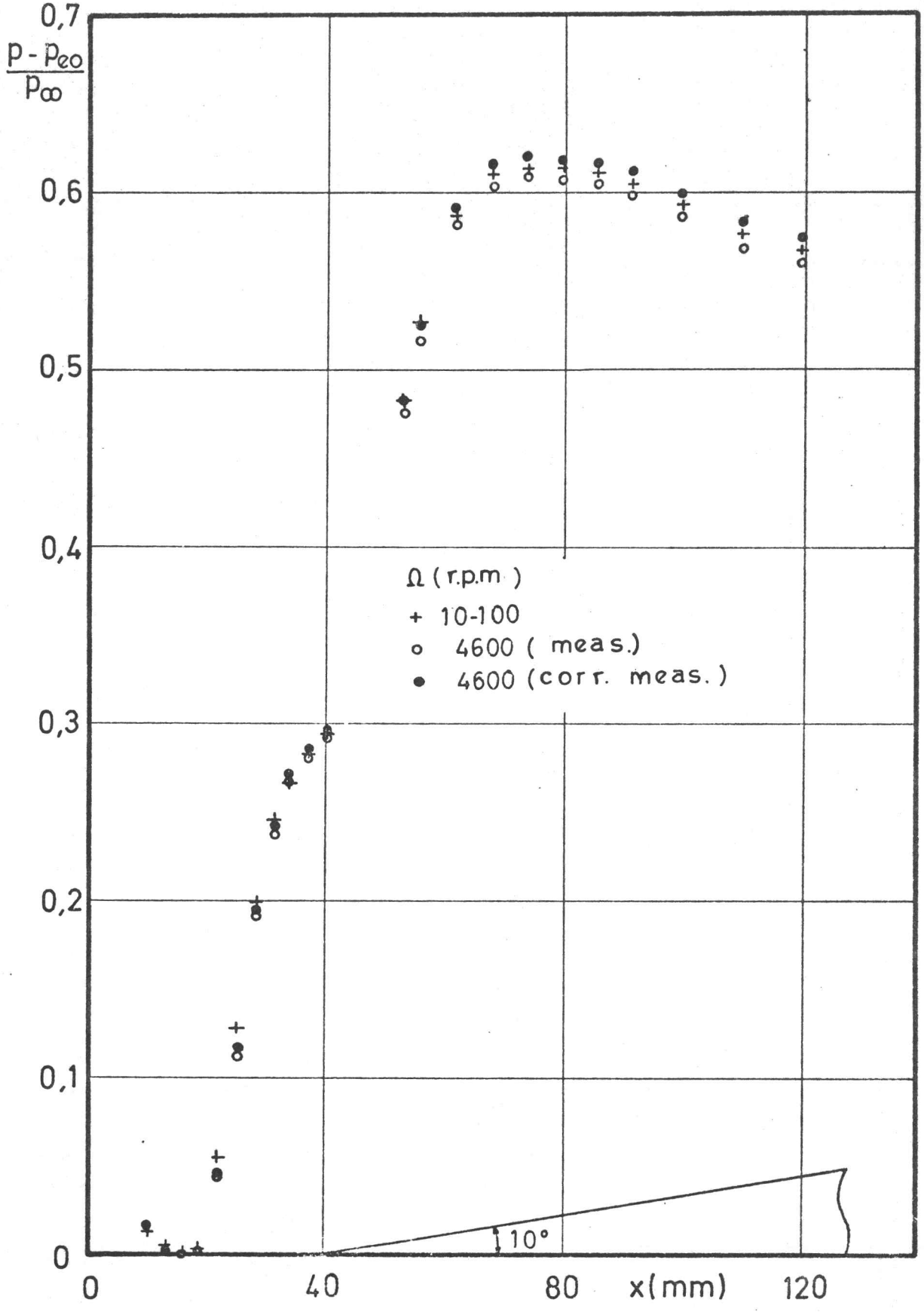

Fig. A_1 - Laminar tendency ($\delta = 7.5°$, $p_t = 97.2$ mmHg)

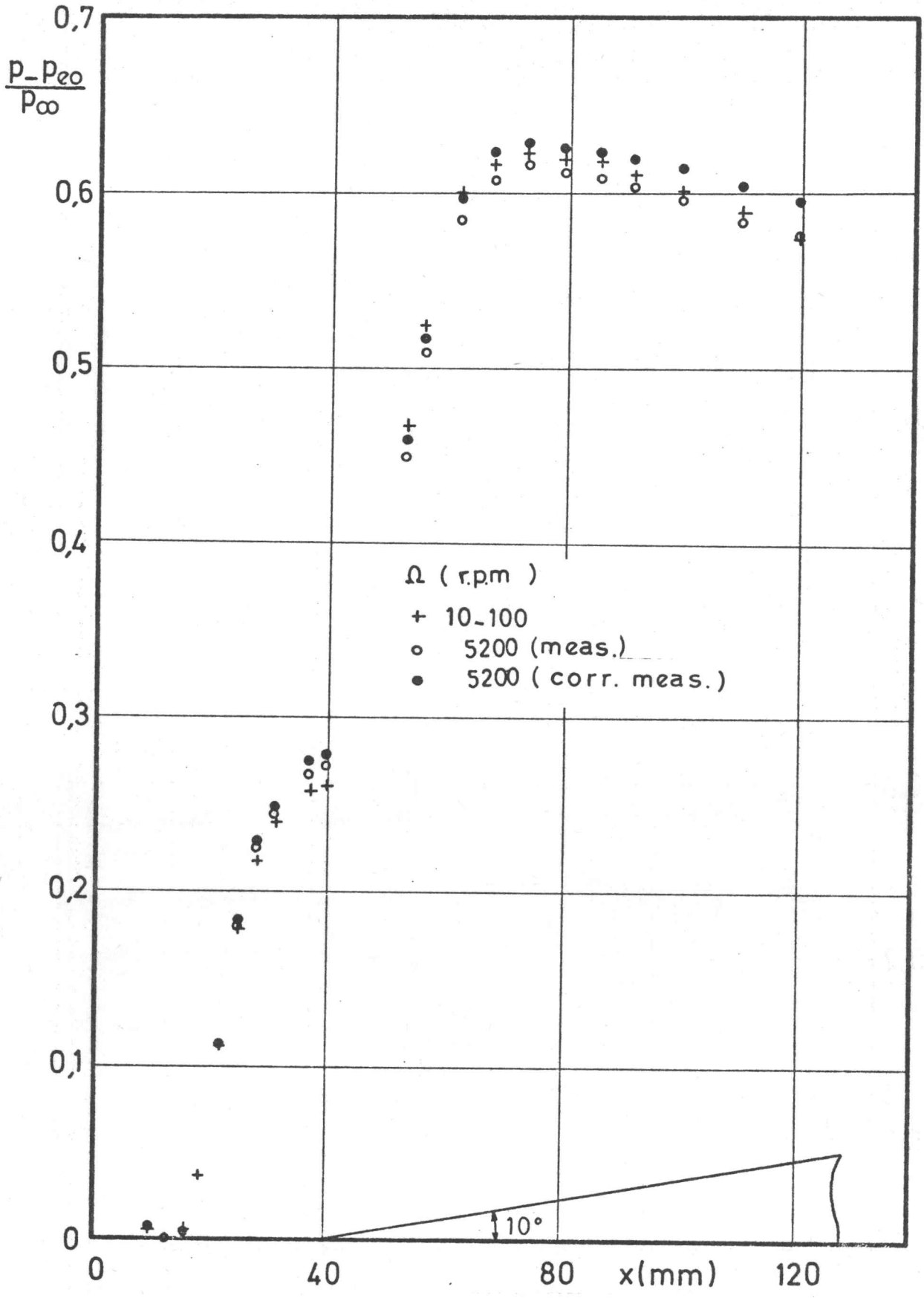

Fig A_2 - Transitional tendency(δ=10°, p_t=172.6 mmHg)

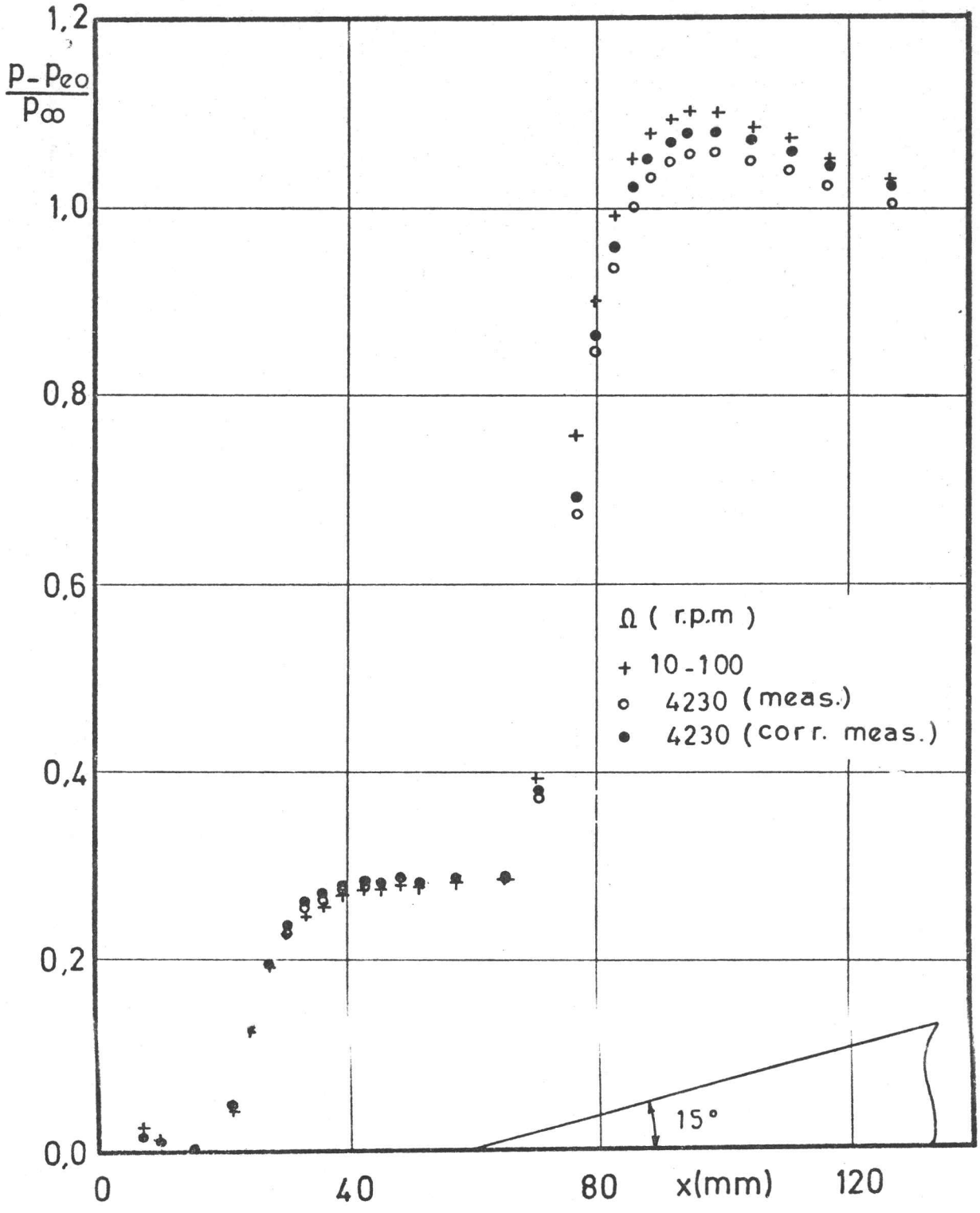

Fig. A_3 - Transitional tendency ($\delta = 15°$, $p_t = 100$ mmHg)